FORSCHUNGSZENTRUM JÜLICH GmbH

Institut für Chemische Technologie

Cold Oxidation of Hydrogen in a Final Nuclear Repository

Jožef J. Čomor

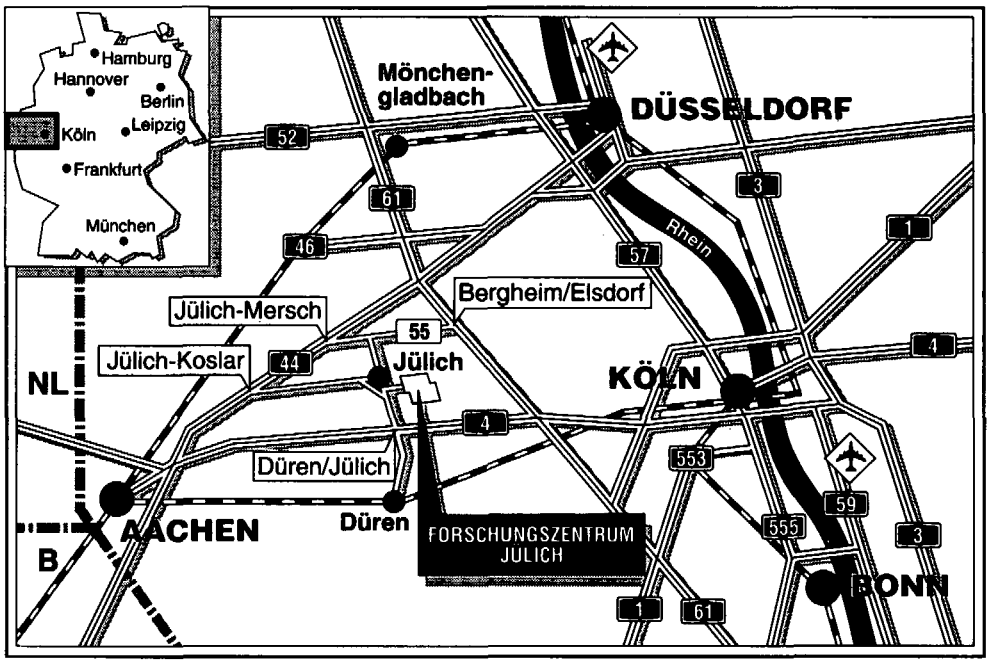

Berichte des Forschungszentrums Jülich ; 2632
ISSN 0366-0885
Institut für Chemische Technologie Jül-2632

Zu beziehen durch: Forschungszentrum Jülich GmbH · Zentralbibliothek
Postfach 1913 · D-5170 Jülich · Bundesrepublik Deutschland
Telefon: 02461/61-6102 · Telefax: 02461/61-6103 · Telex: 833556-70 kfa d

FORSCHUNGSZENTRUM JÜLICH GmbH

KFA

Jül-2632
June 1992
ISSN 0366-0885

Cold Oxidation of Hydrogen in a Final Nuclear Repository

Jožef J. Čomor

Die Arbeit wurde im Rahmen des Vorhabens **MAW- und HTR-BE-Versuchseinlagerung in Bohrlöchern** (Projekt MHV) durchgeführt

Das diesem Bericht zugrundeliegende Vorhaben wurde mit Mitteln des Bundesministers für Forschung und Technologie unter dem Förderkennzeichen KWA 5302 B6 gefördert. Die Verantwortung für den Inhalt dieser Veröffentlichung liegt bei dem Autor.

Work has been carried out at the Forschungszentrum Jülich (KFA) since 1983 on a project for the „Further Development of Borehole Technology for the Disposal of Radioactive Wastes in Salt with the Example of Dissolver Sludge, Cladding Hulls, Structural Components and HTR Fuel Elements". The project is supported by the Bundesminister für Forschung und Technologie (BMFT) under reference number KWA 5302 B6 and known by the short title **„ILW and HTR Fuel Element Test Disposal in Boreholes"** (MHV Project).

The overall goal of the project is to develop methods suitable for the disposal of the above mentioned wastes in boreholes in salt and to test these methods in the Asse salt mine.

The **Institut für Chemische Technologie (ICT)** at the KFA Jülich manages the scientific work and organization of the project.

The Institut für Tieflagerung (IfT) at the Gesellschaft für Strahlen- und Umweltforschung (GSF) is responsible for the geomechanical and mining work involved in the project; this institute monitors the in situ experiments and as the owner of the Asse salt mine it functions as the applicant for the experiments with respect to the licensing authorities.

Geomechanical calculations are carried out by the Bundesanstalt für Geowissenschaften und Rohstoffe (BGR).

The Bundesamt für Strahlenschutz (BfS), the Gesellschaft für Nuklear-Service (GNS), the Deutsche Gesellschaft zum Bau und Betrieb von Endlagern für Abfallstoffe (DBE) as well as the project Hochtemperaturreaktor-Brennstoffkreislauf (HBK) advise the project management and ensure that the boundary conditions of the waste producers and the disposers of the wastes (Gorleben planning) are taken into consideration.

Cold Oxidation of Hydrogen in a Final Nuclear Repository

by Jožef J. Čomor

Abstract

A material was developed to absorb hydrogen during its production in a final repository. The absorption material consists of electrolytically prepared MnO_2 catalytically activated by Ag_2O. The preparation technique of the material was optimized. The kinetics of hydrogen absorption was investigated. The capacity of the material was found to be 0.2 m^3_{STP} H_2/kg MnO_2.

The applicability of the material was shown by a demonstration test simulating the conditions in a rock salt repository.

Key words: manganese dioxide, silver oxide, hydrogen, cold oxidation, intermediate level radioactive waste, rock salt repository

Kaltverbrennung von Wasserstoff in einem nuklearen Endlager

von Jožef J. Čomor

Zusammenfassung

Ein Absorptionsmaterial wurde entwickelt, das den in einem Endlager entstehenden Wasserstoff auf chemischem Wege umsetzt. Bei dem Absorptionsmaterial handelt es sich um elektrolytisch hergestelltes MnO_2, das mit Ag_2O katalytisch aktiviert ist. Das Verfahren zur Herstellung des Materials wurde optimiert. Die Kinetik der H_2-Absorption wurde untersucht. Die Kapazität des Materials wurde ermittelt zu 0,2 Nm^3 H_2/kg MnO_2.

Durch einen Demonstrationsversuch wurde die Anwendbarkeit des Materials unter Bedingungen, die für ein Endlager im Salz typisch sind, nachgewiesen.

Stichworte: Mangandioxid, Silberoxid, Wasserstoff, Kaltverbrennung, Mittelradioktive Abfälle, Endlager im Salz

CONTENTS

1. INTRODUCTION

In the Federal Republic of Germany, it is planned to dispose of intermediate level waste containers with heat production (ILW) in deep vertical boreholes in rock salt. These packages contain reprocessing wastes such as fuel hardware, cladding hulls and dissolver sludge, as well as spent fuel elements which are intended for disposal without reprocessing. The waste materials are fixed in cement-based matrices, according to the practice in the reprocessing plants (WAK, COGEMA, BNFL). As a consequence of high radiation fields inside the containers, the water from the cement matrix will be radiolytically disintegrated and thus these waste packages are certain sources of gaseous hydrogen[1,2]. An additional source of hydrogen is the corrosion of metallic waste constituents and container materials. This released hydrogen, when mixed with air, might form explosive gas mixtures and this is especially critical for the operational safety of the repository. The formation of gases from the waste packages will also lead to unwanted over-pressure in the closed boreholes. The most promising way to overcome this problem is the emplacement in an appropriate form into the borehole of some materials capable of adsorbing or catalytically oxidizing hydrogen. Since hydrogen is a highly inert gas, there is practically no convenient adsorbent that can be used for this purpose in plausible amounts[3]. Application of special catalyst materials (for instance Pd, Pt, Ni) will not solve the problem, since the amount of gaseous O_2 required for cold catalytic oxidation of H_2 is limited in a closed borehole. Apparently, the only solution is to use a solid material as a source of oxygen that can react with H_2 with or without catalytic activation. Several different materials were tested in KFA Jülich[4] and it appears that silver-catalyzed MnO_2 is the most advantageous one. It is well known that numerous silver compounds can catalytically activate MnO_2 for the reaction with hydrogen, even at room temperature[5]. The subject of this investigation is optimization of the preparation technique and testing of the material under repository-relevant conditions.

2. PREPARATION OF ACTIVATED MnO_2

MnO_2 is available on the market in two forms: as a natural ore pyrolusite (brownstone) with purity of 85-90% and as electrolytically prepared, "battery grade", synthetic material with purity greater than 90 %. The main difference between these two materials is in their specific surface area. The powder prepared from natural ore has very low specific surface area, while the synthetic material usually has 15-80 $m^2 \cdot g^{-1}$ [5]. Because of this difference in the amount of the contact surface with gases, one can expect definite differences between the reactivity of these two materials. In order to choose the best material for hydrogen oxidation, both the natural and electrolytic MnO_2 were tested. Many silver compounds are known to be capable of catalytic activation of MnO_2, but Ag_2O and AgO are the most active ones[5].

The reaction rate during heterogeneous catalysis is very much influenced by the contact surface between the catalyst and the reaction materials. To increase this contact area the catalyst particles must be as small as possible. Various preparation techniques were tested in order to optimize the reaction rate, as well as the stability of the reaction material under repository-relevant conditions.

2.1. Natural MnO_2-based materials

Catalytic activation of MnO_2 can be achieved by a simple mixing of powders of MnO_2 and the catalyst and by chemical deposition of catalyst particles on the MnO_2 surface. In the first case, one has to take into account poor contact between the catalyst and the MnO_2 particle, while in the second case, certain complicated preparation techniques must be applied. Since the natural MnO_2 has a rather low specific surface area, the simple powder mixture should result in low reaction rate and therefore all the experiments with natural MnO_2 were carried out with chemically deposited catalyst.

Ag_2O can be easily obtained by the following simple chemical reaction:

$$2Ag^+ + 2OH^- \rightleftharpoons Ag_2O + H_2O \quad . \qquad \text{(Eq. 1)}$$

Ag_2O has low solubility in water (2 mg in 100 g of water at 25 °C) and it is easy to obtain in crystalline form. The dimensions of the Ag_2O particles resulting from the above reaction can be controlled by the concentration of Ag^+ and OH^- ions. The particles will be smaller if the concentrations are lower. The deposition of Ag_2O particles on the surface of MnO_2 was carried out using an apparatus shown in fig. 1. The reaction vessel, **RV**, was filled with a suspension of 25 g MnO_2 (Merck, art. 5957) in 500 ml distilled water. The flow rate through **PTFE** piston dosing pumps

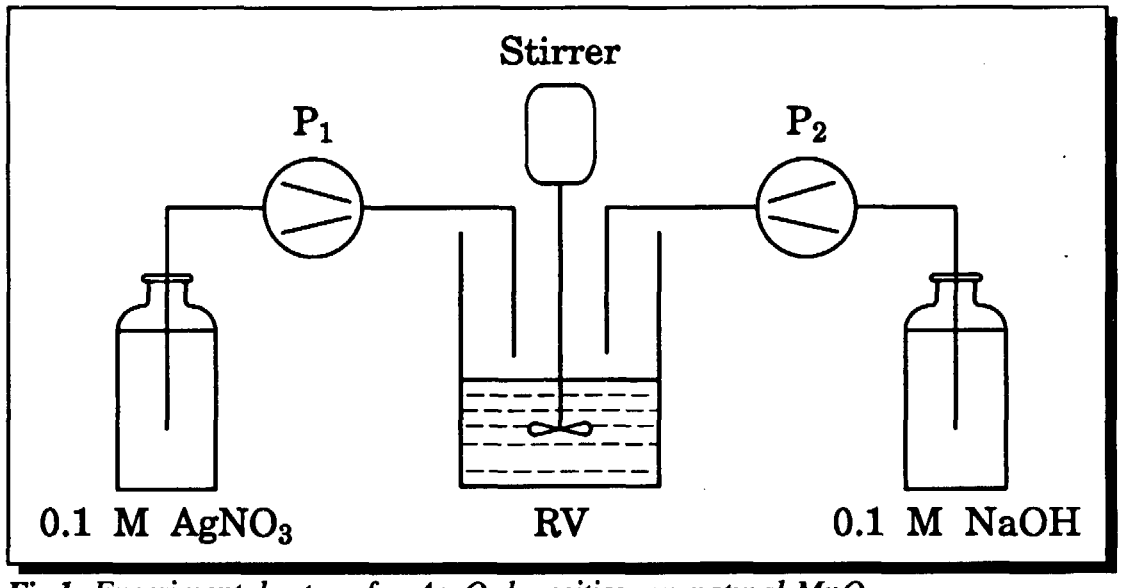

Fig.1. Experimental set-up for Ag_2O deposition on natural MnO_2.

P_1 and P_2 (BF 411/1000, Telab) was adjusted to 1.00 ml·min^{-1} and the 0.1 mol·l^{-1} solutions of $AgNO_3$ and NaOH were pumped simultaneously. As a result, the concentration of both Ag^+ and OH^- ions in the reaction vessel was not much higher than that determined by the solubility of Ag_2O and it was to be expected that the dimensions of the particles would be rather small. After deposition of the desired amount of Ag_2O on the surface of MnO_2, the solid phase was left to settle down, the liquid was removed by decantation and the MnO_2 with deposited Ag_2O was washed several times with distilled water in order to remove all the Na^+ and NO_3^-

ions. Finally, the material was dried at 105 °C for 2 hours. The dimensions of Ag_2O particles on the surface of MnO_2 were determined by combined scanning electron microscope/X-ray analysis (JEOL JSM-840) and it was found that the diameters of the particles were ≤ 1 μm. The amount of Ag_2O deposited on the surface of MnO_2 was controlled by the total volume of $AgNO_3$ and NaOH solutions pumped in the reaction vessel. Samples containing 1 and 1.5 % Ag_2O were prepared. The concentration of Ag_2O was checked by ICP analyses of the material (ARL 3520B ICP analyzer) and it was found that there was no significant difference between the designated concentrations and those determined by ICP.

2.2. Electrolytically prepared MnO_2-based materials

The material used throughout these experiments was electrolytically prepared MnO_2 (Merck, art. 805958). Since one can expect much higher reactivity with this material than with the natural one[5], both possible ways of preparation (powder mixture and chemical deposition) were tested.

2.2.1. Preparation of the active material by powder mixing

The Ag_2O powder was prepared by mixing equal amounts of 0.1 M $AgNO_3$ and 0.1 M NaOH solutions. After the Ag_2O had settled down, the liquid phase was removed by decantation and the solid material was washed several times with distilled water. Finally, the material was dried at 105 °C for 2 hours.

In order to obtain 100 g of activated material with 1% of Ag_2O, it was necessary to mix 99 g of electrolytically prepared MnO_2, 1 g of Ag_2O powder and 30 ml distilled water until a homogeneous sludge was obtained (10 - 15 min.). The role of the water was to improve contact between the Ag_2O and MnO_2 particles. After homogenization, the sludge was dried at 105 °C overnight. After drying, the material was compacted and it was necessary to grind it until a fine powder was obtained. Materials containing 0.25, 0.50, 0.75, 1.00 and 10% of Ag_2O were prepared using this technique.

2.2.2. Deposition of Ag^+ by ion exchange

It is well known that electrolytically prepared MnO_2 has ion exchange capabilities[6]. Fig 2 shows the ion exchange isotherms of Ag^+, K^+, Ca^{2+} and Mg^{2+} ions. These results were acquired by equilibration of 10 ml of 0.1 M solutions of $AgNO_3$, K_2SO_4, $Ca(NO_3)_2$ and $Mg(NO_3)_2$ with various quantities (1 - 25 g) of electrolytic MnO_2 at room temperature. The exchanged amounts of the ions were calculated from the difference between their starting and end concentrations in the water phase, analyzed by ICP. To prove that it really was ion exchange and not simply adsorption, the pH of the solutions was measured before and after equilibration. In each case, the pH after equilibration was lower than in the starting solution indicating that the metal ions in the solution were replaced by H^+ ions

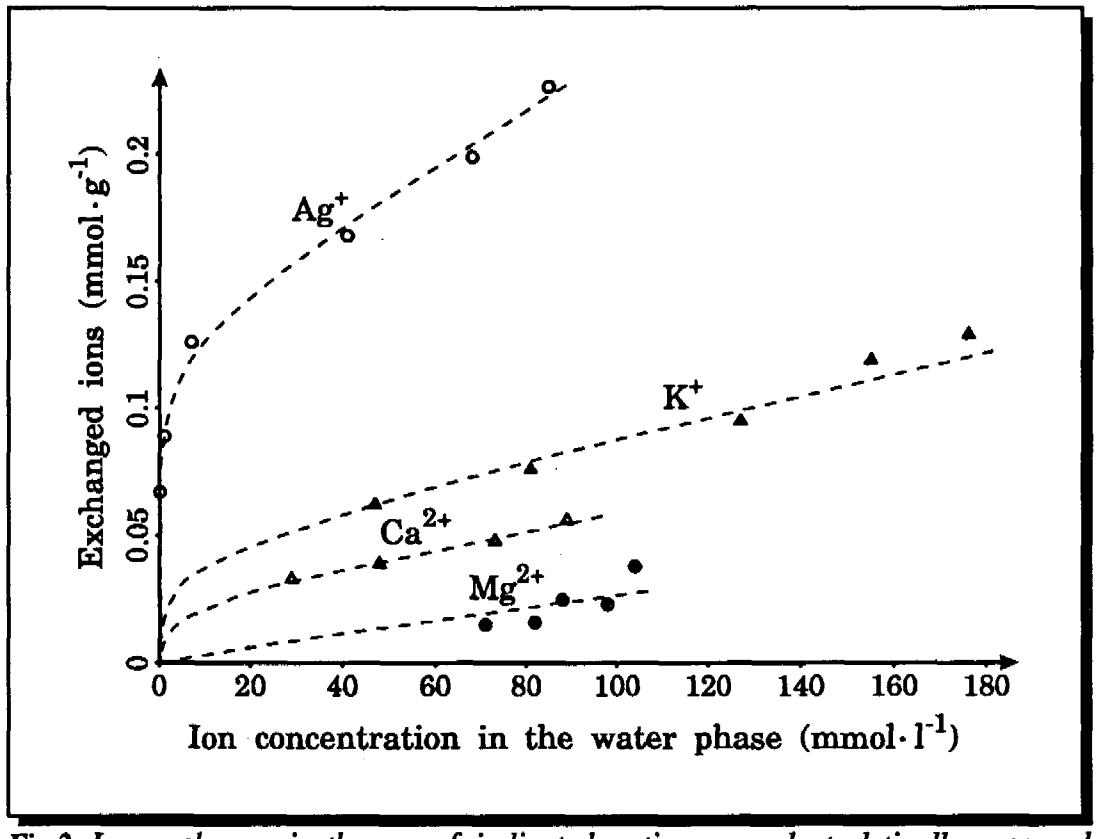

Fig.2. Ion exchange isotherms of indicated cations on electrolytically prepared MnO_2 at room temperature.

coming from the surface of MnO_2. The ion exchange centers were most probably the strongly bonded -OH groups on the surface of MnO_2[7] and the reaction is as follows:

$$Bulk\text{-}OH + M^+ \rightleftharpoons Bulk\text{-}OM + H^+ . \qquad \text{(Eq. 2)}$$

From the ion exchange isotherm of Ag^+ ion on MnO_2 (fig. 2.), the ratio can be estimated at which the solution of $AgNO_3$ should be mixed with MnO_2 powder in order to obtain a desired concentration of Ag on the surface of MnO_2. The material containing 1.0% Ag was prepared by mixing 1020 ml 0.01 M $AgNO_3$ with 99 g of electrolytic MnO_2. After equilibration (mixing for 10 min.), the liquid phase was removed by decantation and the material was dried in vacuum at room temperature. This starting material was later variously modified by chemical or thermal treatment. Electron microscope/X-ray analysis of this material showed that the silver was homogeneously distributed on the surface of MnO_2 particles without any definite Ag particles, once more emphasizing that the bonding mechanism of Ag to the MnO_2 was by ion exchange.

2.2.3. Modification of the material prepared by ion exchange

In order to obtain small clusters of Ag_2O on the surface of MnO_2, the material prepared by ion exchange was treated by 0.1 M solutions of NaOH or Na_2CO_3. Ion exchange is a reversible process and consequently there are always Ag^+ ions in the water phase in equilibrium with the bonded ions on the surface. Ag_2O will be produced by addition of OH^- ions to the water phase, decreasing the concentration of Ag^+ in the water phase. Since the equilibrium is thus disturbed, additional Ag^+ ions will be removed from the surface of MnO_2. If the concentration of OH^- is high enough, the transformation to Ag_2O will occur practically on the surface of MnO_2, preventing the formation of large Ag_2O crystals. In the case of treatment with Na_2CO_3 solution, the result will be the formation of Ag_2CO_3 clusters. Ag_2CO_3 is quite an unstable compound and it can be destroyed even by drying the material at 105 °C, if the particles are very small, according to the reaction:

$$Ag_2CO_3 \rightarrow Ag_2O + CO_2 \ . \qquad \text{(Eq. 3)}$$

The chemical modification was carried out by mixing 100 g of the material prepared by ion exchange with 200 ml of 0.1 M solution of NaOH (or Na_2CO_3) at room temperature for 20 min. After the solid settled down, the liquid was removed by decantation and the material was rinsed once with distilled water. Then it was dried in vacuum at room temperature. Electron microscope/X-ray analysis of the samples showed that the silver was still homogeneously distributed on the surface of MnO_2 with no definite Ag_2O particles, meaning that the diameters of the clusters were less than 100 nm.

The samples prepared by ion exchange and the chemically modified samples were further thermally (24 hours at 105, 210, 300 or 400 °C) or chemically (48 hours in contact with saturated solutions of NaCl or Na_2S) treated, in order to deactivate the material.

3. KINETICS OF THE H_2 + ACTIVATED MNO_2 REACTION

The simplest way to measure the reaction rate between a gas and a solid is (when the reaction products are not gases) to measure the gas pressure. The

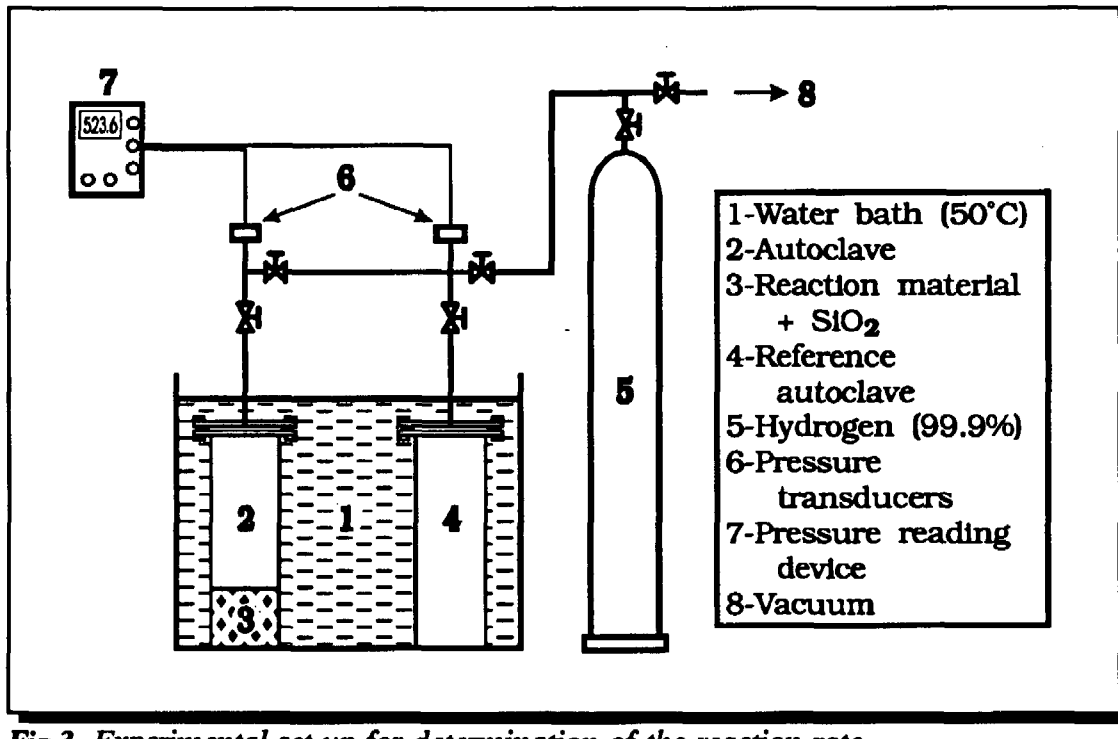

Fig.3. Experimental set-up for determination of the reaction rate.

experimental set-up used throughout these measurements is shown in fig. 3. Two autoclaves made from stainless steel with an inner volume of 1700 ml were thermostated in a water bath. One autoclave was used as a source of hydrogen during the filling procedure of the other autoclave containing the reaction material. The hydrogen used during the measurements was of 99.9% purity. The pressure was measured by precise pressure transducers (P42 P, Hottinger Baldwin Messtechnik) in the range from 0 to 2 bars, with a resolution of 0.1 mbar and linearity better than

0.3%. The temperature in the water bath was controlled by an immersion thermostat (HAAKE E51) with a precision of 0.05 °C.

The mechanism of the reaction between H_2 and activated MnO_2 is not strictly known, but there are some indications that it takes the following route[5]. Physically adsorbed hydrogen dissociates at the contact point between the Ag_2O and MnO_2 particles:

$$H_2 \rightleftharpoons 2H^{\cdot} \quad . \qquad \text{(Eq. 4)}$$

These hydrogen radicals can then react with MnO_2 according to the reaction:

$$2H^{\cdot} + 2MnO_2 \rightleftharpoons Mn_2O_3 + H_2O \quad . \qquad \text{(Eq. 5)}$$

This reaction seems to be favored on the surface of the MnO_2 crystal, from where the H_2O molecule can leave. It is well known that hydrogen radicals can be easily injected into the bulk of many crystals and one can expect that the reaction in the bulk is[5]:

$$H^{\cdot} + MnO_2 \rightleftharpoons H_xMnO_2 \qquad \text{(Eq. 6)}$$

since the H_2O molecule is too large to be able to leave the bulk of the MnO_2 crystal.

The total pressure during the reaction can be affected by the water vapor pressure and therefore some dry silica gel was added to the reaction vessel in order to adsorb all the water formed. The reaction material (activated MnO_2) was usually mixed with SiO_2 in a 1:1 mass ratio. All the kinetic experiments were carried out at 50.0 °C in the following way. The autoclave was filled with a mixture of 100 g activated material and 100 g SiO_2, closed and immersed in the thermostated bath and evacuated overnight in order to clean the surface of the material from all adsorbed gases. Then, the autoclave was filled with H_2 up to about 500 mbar and the pressure was recorded as a function of time. The reaction rate was calculated from these functions, as will be described later on. When a very fast reaction was

expected, filling was carried out using the reference autoclave. This was evacuated, filled with H_2 up to 1000 mbar and then equilibrated with the reaction autoclave for 5 sec. The initial pressure in the reaction autoclave was then calculated from the pressure drop in the reference autoclave. After all the hydrogen had been absorbed, the autoclave was again refilled with H_2. In order to measure the reaction rate of the material which had experienced significant losses to its capacity, the pressure transducers were replaced by manometers and the autoclave was filled with H_2 up to 5 - 10 bars. The amount of the reacted hydrogen was calculated from the pressure drop. Then, the manometers were replaced by the transducers, the autoclaves were evacuated and the procedure described previously was repeated.

3.1. The reaction rate with natural MnO_2

Bearing in mind that the reaction occurs between a gas and a solid, one would expect a perfect first order reaction, for which the reaction rate is a linear function of pressure

$$-\frac{dp}{dt} = kp \ . \qquad \text{(Eq. 7)}$$

The solution of that differential equation is

$$p = p_o e^{-kt} \qquad \text{(Eq. 8)}$$

or after logarithm

$$\ln p = \ln p_o - kt \ . \qquad \text{(Eq. 9)}$$

Fig. 4 shows a typical pressure drop (on a semi-logarithmic scale) in the autoclave as a function of time. As one can see, the functionality differs slightly from a straight line, suggesting that the reaction is not a perfect first order one, but a pseudo-first order reaction. That means that the reaction constant **k** in eqs. 7-9 is a function of the remaining capacity of the solid material, instead of a real constant value. Assuming that the overall reaction is

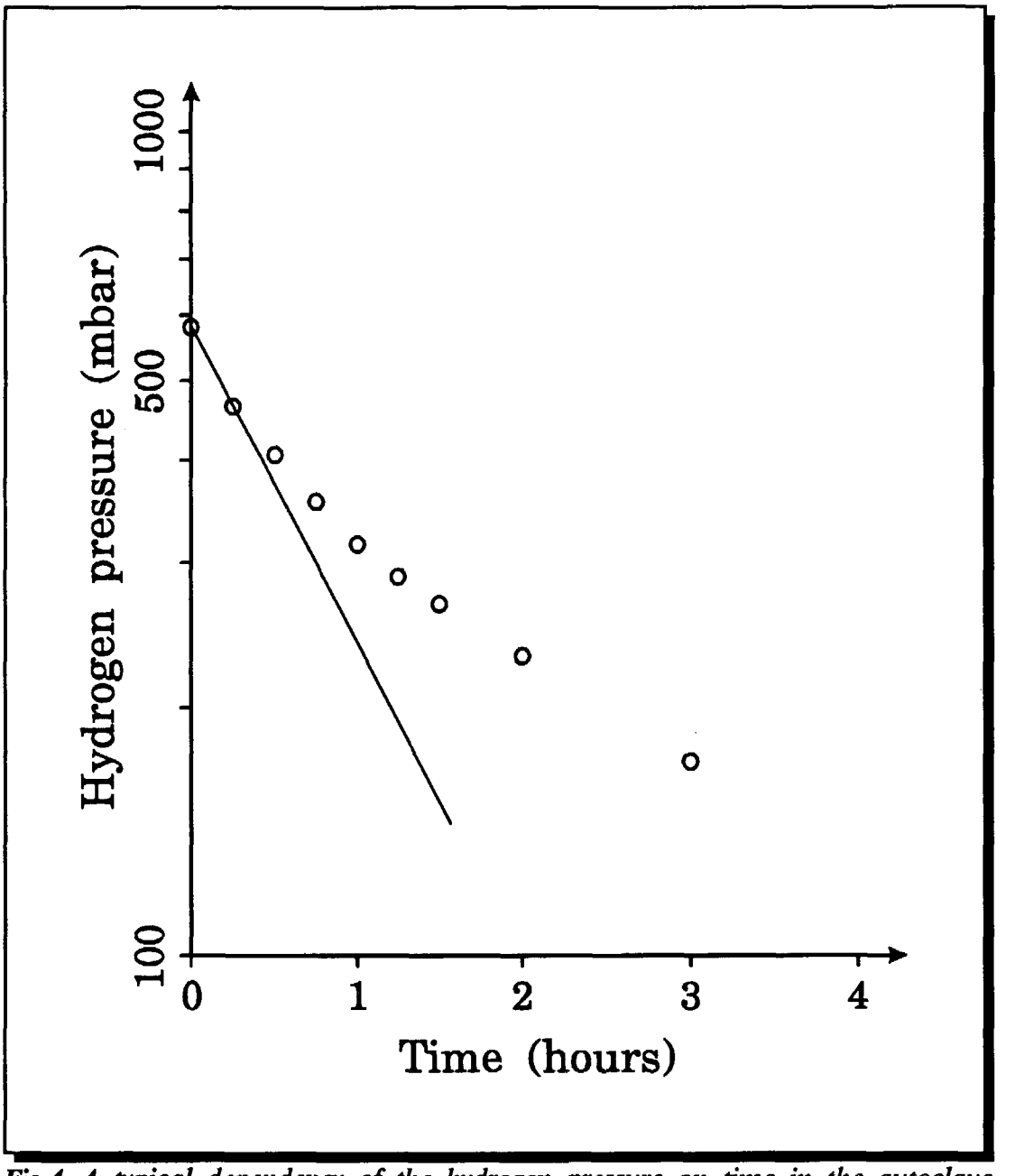

Fig.4. A typical dependency of the hydrogen pressure on time in the autoclave containing activated MnO_2.

$$H_2 + 2MnO_2 \rightleftharpoons Mn_2O_3 + H_2O \quad , \qquad \text{(Eq. 10)}$$

the total capacity of 1 mol MnO_2 is 1/2 mol H_2. Quite arbitrarily, one can say that the age of the fresh MnO_2 is 0% and that the age of the completely reduced MnO_2 (up to Mn_2O_3 or $HMnO_2$) is 100%. In this case, the reaction constant for the fresh

material (age = 0%) is k_0 and the reaction constant for the reduced material (age = 100%) is 0. Between these two boundary cases, the reaction constant follows some functionality

$$k = k(a) \quad \{k(0)=k_o,\ k(100)=0\} \qquad \text{(Eq. 11)}$$

where **a** stands for the materials' age. The theoretical evaluation of that functionality is not possible without knowing all the details of the reaction mechanism, but it can be experimentally obtained. Combination of eqs. 7 and 11 results in

$$k(a) = -\frac{1}{p}\frac{dp}{dt} = -\frac{1}{p}\frac{\Delta p}{\Delta t} \qquad \text{(Eq. 12)}$$

allowing us to calculate the reaction rate from the rate of the pressure drop in the reaction vessel, while the age of the material can be calculated from the total pressure loss, assuming that hydrogen is an ideal gas:

$$a = \frac{2(p_o - p)VM}{RTm}100 \qquad \text{(Eq. 13)}$$

where p_0 is the starting hydrogen pressure, **p** is the actual pressure, **V** is the free volume of the system, **M** is the molecular mass of the material (M_{MnO2} = 86.94), **R** is the gas constant (**R** = 8.314 $J \cdot mol^{-1}$), **T** is the temperature of the system and **m** is the mass of the MnO_2 in the closed system.

Fig. 5 shows the dependency of the reaction rate constant on the age for three different materials. At the beginning, the reaction constant decreases rapidly as the material looses its capacity. After an age of ≈10% is reached, the reduction begins to be rather slow, becoming practically a linear function of the age. The difference between the materials with 1.5% (open circles) and with 1% Ag_2O (solid circles in fig. 5) is evident. Higher Ag_2O concentration results in higher reaction rate. There is also a difference in the total capacity of the two materials. For those with 1.5% Ag_2O, the total capacity is ≈110%, meaning that some of the Mn_2O_3 (or $HMnO_2$) can be further reduced (H_xMnO_2, x>1). The total capacity of the material

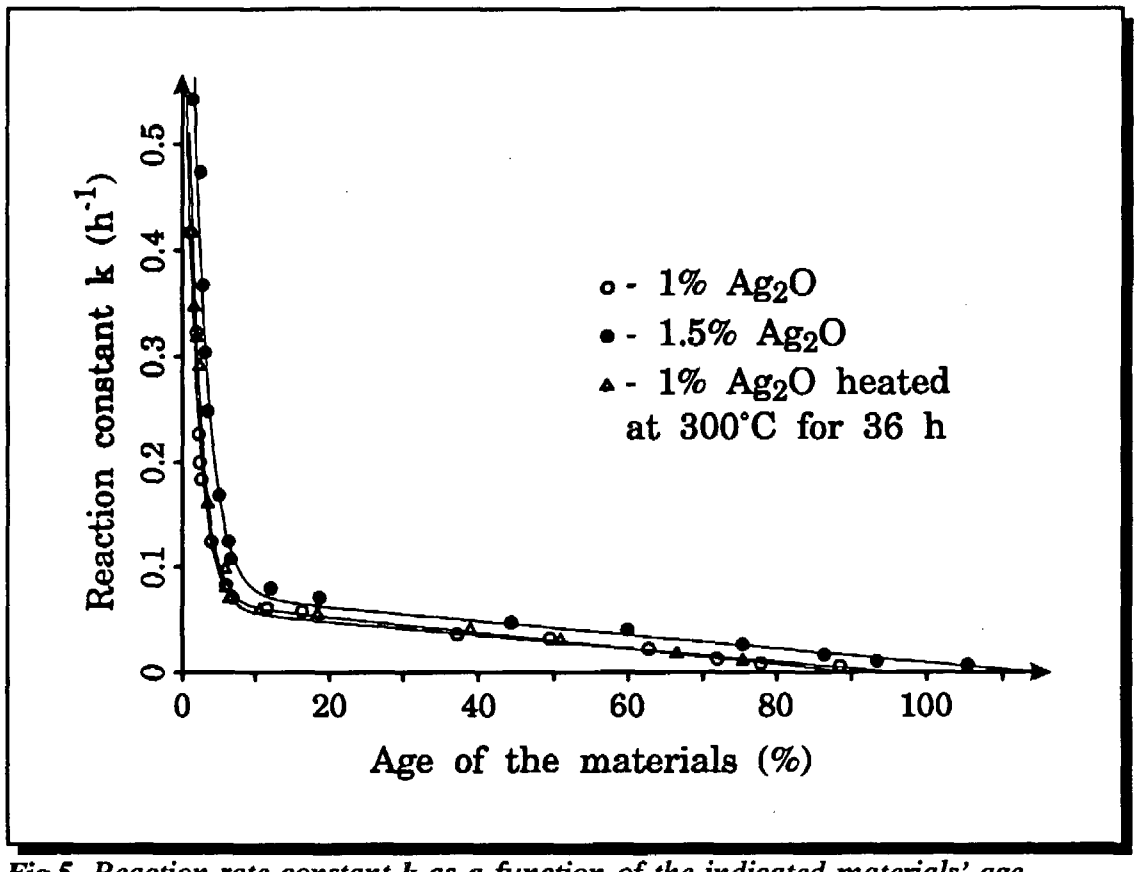

Fig.5. Reaction rate constant k as a function of the indicated materials' age.

containing 1% Ag_2O is ≈90%, probably because there are some MnO_2 particles without Ag_2O particles on the surface. The third material in fig. 5 is MnO_2 with 1% Ag_2O, heated at 300 °C for 36 hours (open triangles). The reason for that treatment was to increase the decomposition rate of Ag_2O according to the reaction

$$2Ag_2O \rightarrow 4Ag + O_2 \qquad \text{(Eq. 14)}$$

and to evaluate the catalytic activity of metallic Ag particles. This is important, since Ag_2O can be decomposed even at lower temperatures, but at significantly slower rate and that could influence the applicability of the material on a very long term scale. As one can see, there is no significant difference between the heated and untreated materials, demonstrating that in the case of natural MnO_2 the catalytic activity of Ag_2O and Ag is practically the same. A possible reason for that effect is, that the surface of metallic silver is always covered by a thin film of oxide, which prevents further oxidation of the bulk. Probably, a film of Ag_2O can have the same

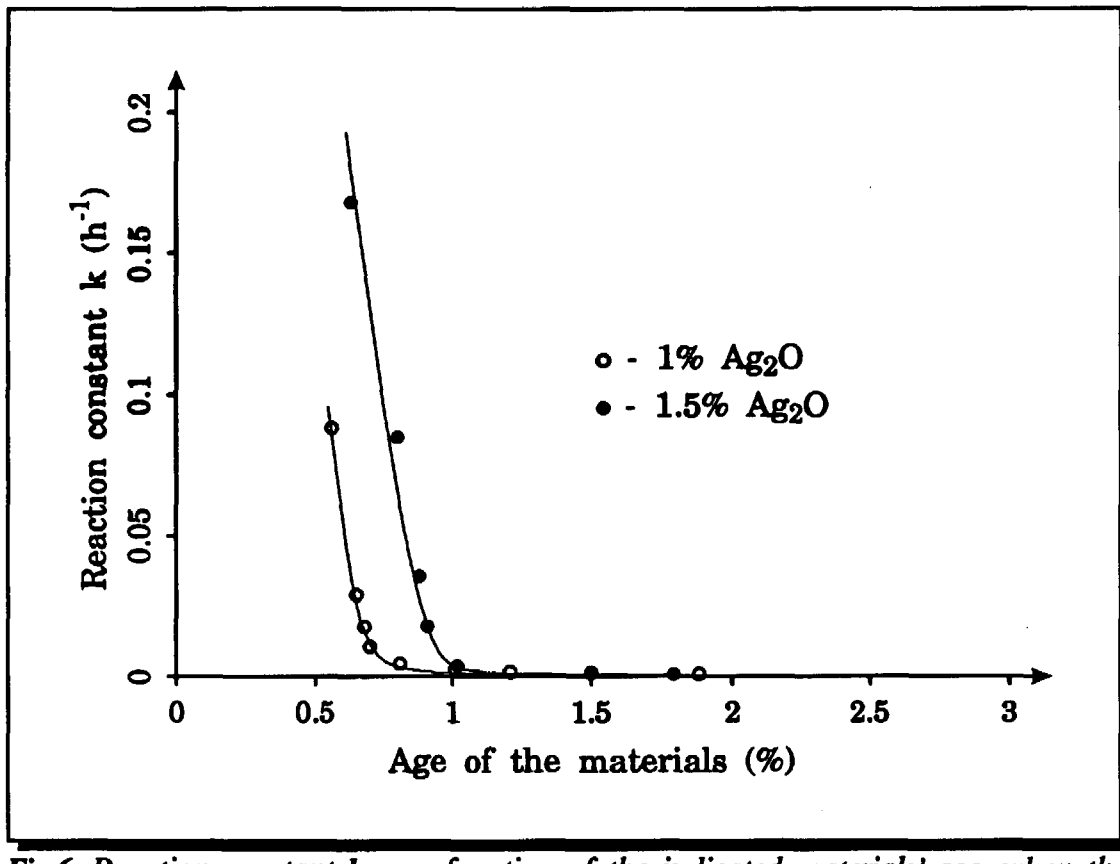

Fig.6. Reaction constant k as a function of the indicated materials' age, when the atmosphere is saturated with water vapor.

catalytic activity as an Ag_2O particle.

The presence of humidity cannot be excluded from a borehole in rock salt. Therefore, it is necessary to evaluate the possible influence of humidity on the reactivity of the activated MnO_2. Since water is a reaction product, the only way to carry out such a measurement is under an atmosphere saturated by water vapor. The autoclave was filled with 100 g of reaction material and a beaker containing 100 ml of distilled water was inserted into the autoclave (the reaction material had no direct contact with the liquid). The system was then evacuated, in order to remove the air, for 2 hours. Part of the water was also removed, since the water vapor pressure at 50 °C is ≈123 mbar. Then, the system was left overnight in order to saturate the atmosphere and the surface of MnO_2 with water. The autoclave was then filled with H_2 up to 500 mbar and the reaction constant and the age of the material were calculated from the pressure drop. Fig. 6 shows the reaction constants

of the materials containing 1 (open circles) and 1.5% Ag_2O (solid circles), as a function of the materials' age, when the gas phase is saturated with water vapor. The starting reaction rate is much less than under dry conditions and there are many reasons for this. If the surface of the solid material is covered by a thin film of water, the reaction rate must be influenced by the solubility of H_2 in water, by the diffusion constant of H_2 in water and by possible chemical influences on the catalytic behavior of the Ag_2O/MnO_2 contact. Since the reaction was practically stopped at age ≈2%, one can conclude that the chemical influence is the most important one. There were probably some places on the crystals that were not completely covered by water film (crystal edges for instance) where the reaction occurred normally. Since the gas atmosphere was saturated with H_2O, the water resulting from the reaction was not able to leave the surface and that completed the covering water film. The result was termination of the reaction.

This is a serious disadvantage of activated natural MnO_2, therefore it is not recommended as a hydrogen absorber under wet conditions.

3.2. The reaction rate with electrolytic MnO_2

Reaction materials based on electrolytic MnO_2 were prepared using two techniques: by powder mixing and by ion exchange. Materials prepared by ion exchange were later variously treated (applying high temperatures or chemical modifiers) in order to obtain a material that can react with hydrogen as fast as possible and the results of these preparation techniques will be discussed separately.

3.2.1. Reactivity of the materials prepared by powder mixing

Fig. 7 depicts experimentally obtained reaction constants of the materials containing 0.25, 0.50, 0.75 and 1.00% Ag_2O as a function of the materials' age. Comparing these curves with the curves from fig. 5 (showing the reactivity of natural MnO_2), several conclusions can be drawn. First, the general shape of the curves is the same: the reaction slows down rapidly while the material is relatively fresh and

after reaching some critical value (which depends on the Ag_2O concentration) the

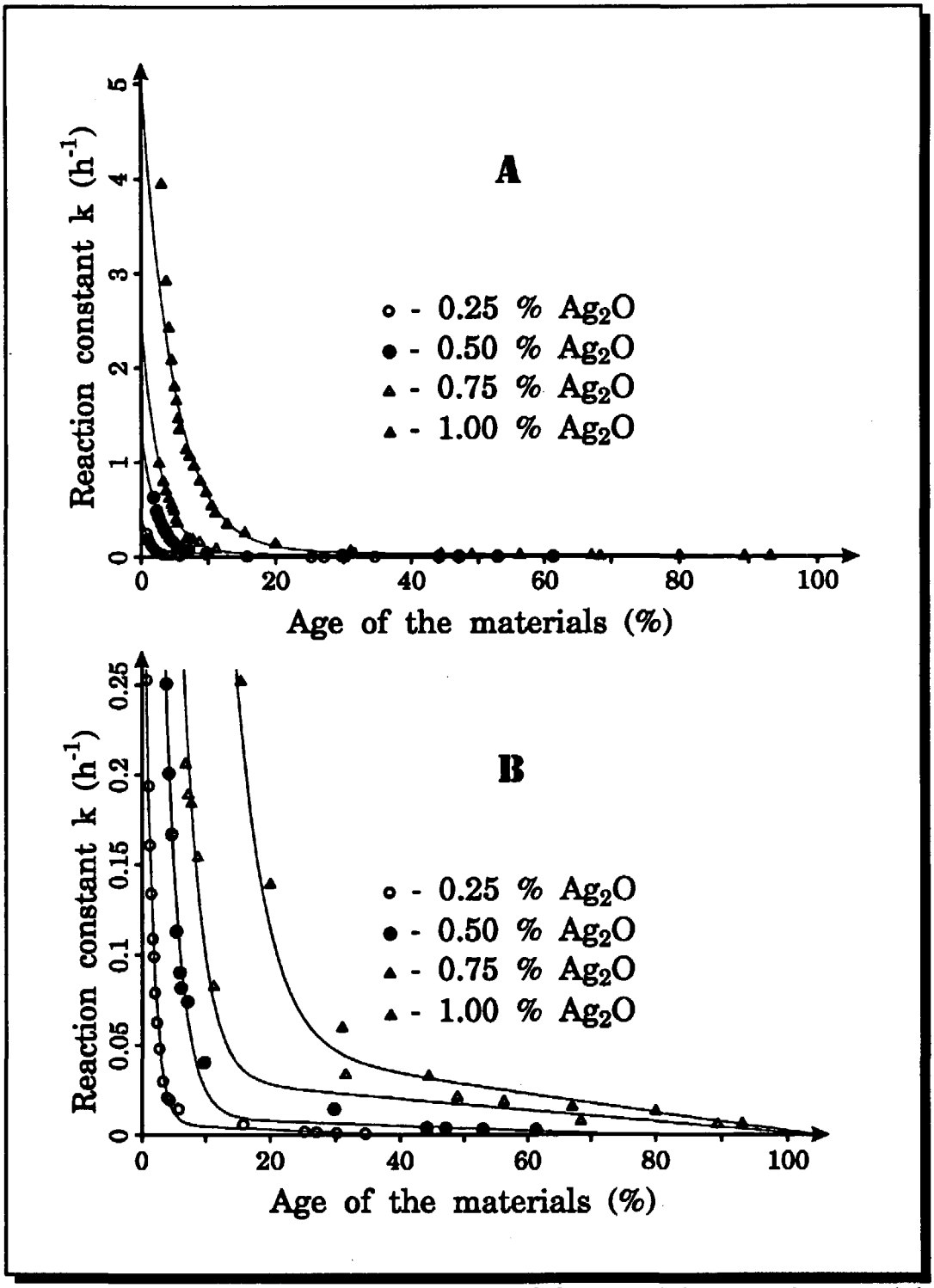

Fig.7. Reaction rate constant as a function of the materials' age. The materials were prepared by powder mixing, with indicated amounts of Ag_2O. Fig. B is the enlarged lower part of fig. A.

curve becomes linear. Second, the initial reaction rate of the electrolytic MnO_2 containing the same amount of Ag_2O is about ten times higher than the reaction rate of natural MnO_2. This difference can be expected knowing that electrolytic MnO_2 has a significantly higher specific surface area and thus a larger reaction area. Third, the reaction with electrolytic MnO_2 is somewhat slower in the linear range of the reaction rate curve indicating that the smaller chemically deposited Ag_2O particles on the surface of natural MnO_2 are more efficient for injection of the hydrogen radicals in the bulk. Finally, there is a certain connection between the materials' capacity, the overall reaction rate and the Ag_2O content: the higher the Ag_2O concentration is, the higher are the reaction rates and the capacity of the materials. If the total available capacity of MnO_2 is needed, at least 0.75% Ag_2O should be mixed with electrolytic MnO_2. Although the initial reaction rate is much higher than with natural MnO_2, the final 70% of the material will react more slowly than the natural MnO_2 with chemically deposited Ag_2O particles on the surface and therefore one can conclude that the powder mixing preparation technique is not an optimal method.

3.2.2. Reactivity of the materials prepared by ion exchange

Fig. 8 depicts the reaction rate constants of the materials prepared by ion exchange (containing 1% Ag) and then dried under different conditions. The material dried in vacuum at room temperature had the highest initial reaction rate, which is about 20 times faster than with natural MnO_2 and about 2 times faster than with the material prepared by powder mixing. Also, in the linear part of the curve, the reaction is significantly faster than with the other two types of materials. The initial reaction rate of the material dried at 105 °C is about half of the vacuum dried material, but upon reaching the age of about 30% the reaction rates become equal. Also, there is no significant difference in the total capacity of these two materials, about 180%, indicating that the MnO_2 is reduced almost completely to MnO (or H_2MnO_2). The difference in the initial reaction rate of these two materials can be a result of some promotion effect of strongly adsorbed H_2O and -OH groups on the

surface of MnO_2. After drying at 105 °C most of the water is removed from the

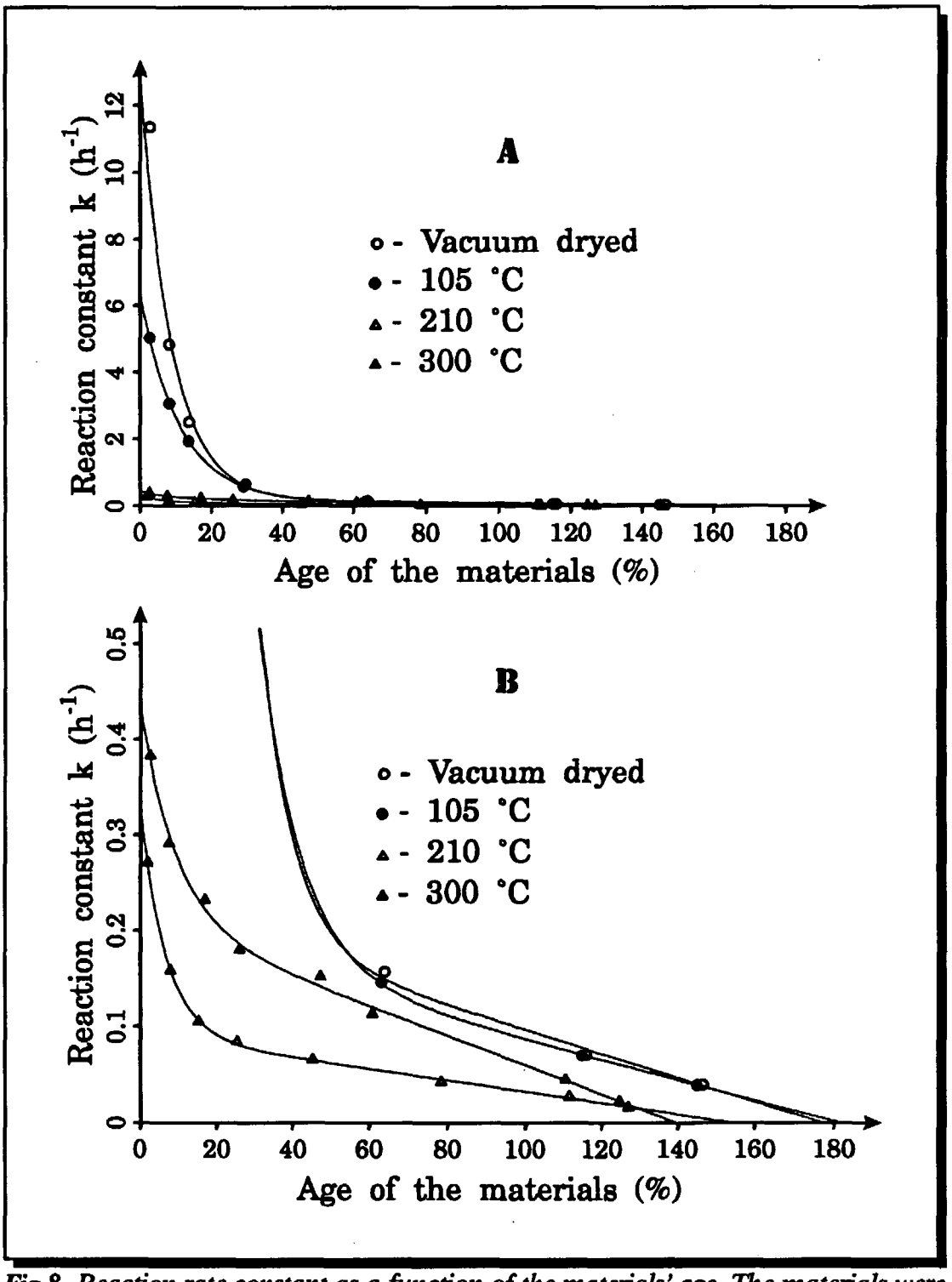

Fig.8. Reaction rate constant as a function of the materials' age. The materials were prepared by ion exchange and dried in different ways. Fig. B is the enlarged lower part of fig. A.

surface and therefore the reaction is somewhat slower. Since water is the product of the reaction between H_2 and MnO_2, the missing H_2O will be replaced and the material will react as if it had been dried in vacuum. The reaction rates with materials dried at 210 and 300 °C are significantly slower, but the curves still have the same shape. The reason for the slowing down of the reaction could be some thermal degradation of the surface of electrolytically prepared MnO_2 and possible agglomeration of Ag atoms.

3.2.3. Reactivity of chemically modified materials

Fig. 9 shows the reaction rate constants of the materials prepared by ion exchange, further treated by 0.1 M solutions of NaOH or Na_2CO_3 and then variously dried. As one can see, the material treated by NaOH and then dried in vacuum at room temperature had the highest initial reaction rate compared to all other tested materials. That fact nicely fits to the previous conclusion that the -OH groups can have some promotion effect on the reaction since, after treatment with NaOH, not only the Ag is converted to Ag_2O clusters (subsection 2.2.3.), but also the surface of MnO_2 is enriched with adsorbed -OH groups. Comparing the curves obtained with materials treated by NaOH (solid circles) and by Na_2CO_3 (open squares in fig. 9.), one can conclude that there is no significant difference between these two materials, meaning that the pH value of the solution used for treatment is not critical. The total capacity of the materials treated with NaOH and Na_2CO_3 is also the same and it is rather high at about 160%. The materials dried at 210 and 300 °C react similarly and that once more stresses the fact that the water and most of -OH groups are already removed at 200 °C. The initial reaction rate of these two materials is much lower than that of the materials heated up to 105 °C, but the linear parts of all of the curves are almost the same. The capacity of these two materials is again practically the same, somewhat lower than the capacity of the materials treated below 200 °C, amounting to about 130%.

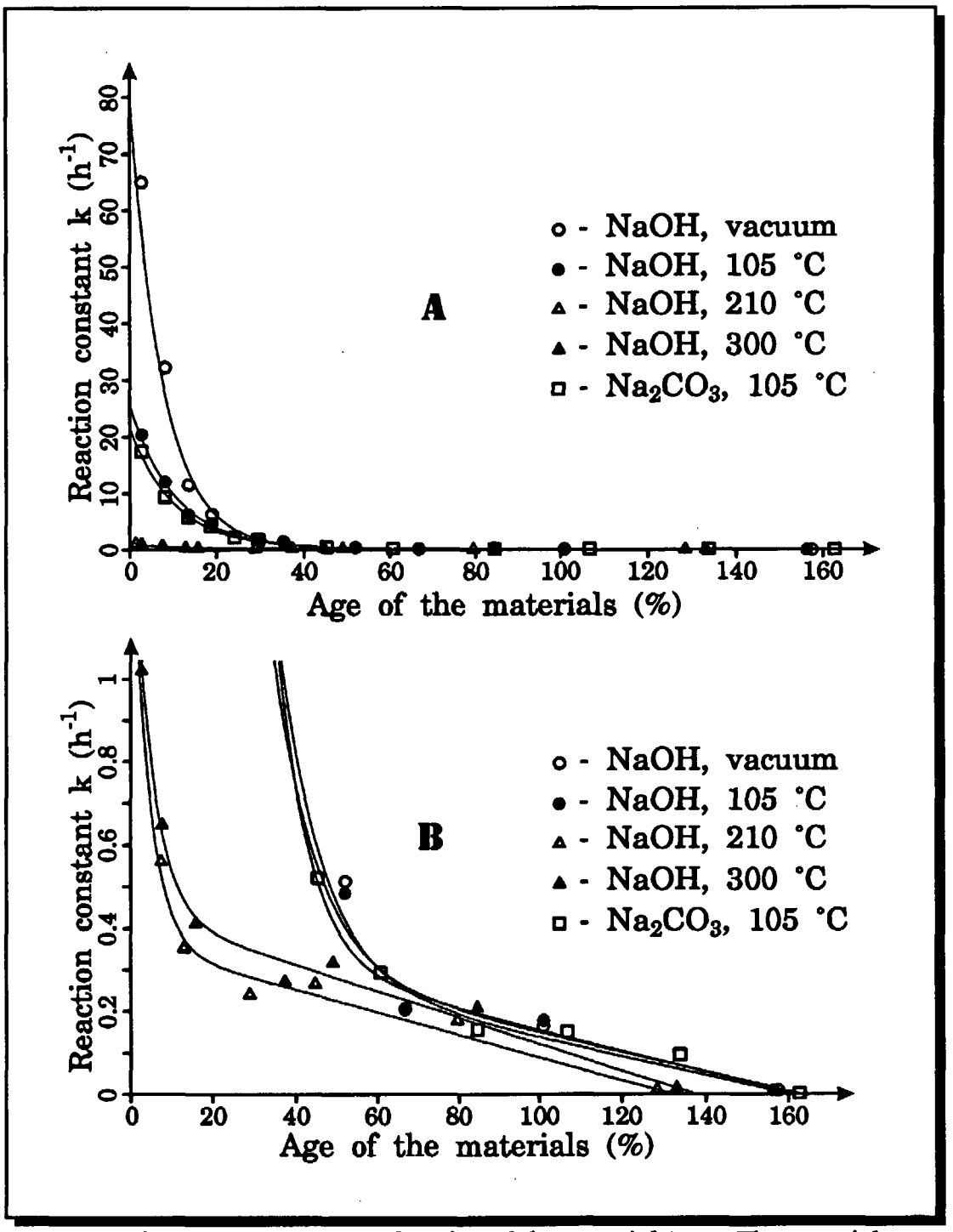

Fig.9. Reaction rate constant as a function of the materials' age. The materials were prepared by ion exchange, chemically treated and dried under different conditions. Fig. B is the enlarged lower part of fig. A.

4. TESTING OF THE REACTION MATERIAL UNDER REPOSITORY-RELEVANT CONDITIONS

Considering the results of testing the reactivity of the materials prepared by different techniques, the material prepared by ion exchange deposition of Ag on the surface of electrolytic MnO_2, further treated with 0.1 M NaOH solution and dried at 105 °C was selected as a reference material for all other tests simulating conditions in the final repository. Although material prepared in the same way but dried in vacuum at room temperature has a much higher initial reaction rate, it is not preferred since drying at elevated temperatures is technically much simpler than vacuum drying.

4.1. Reactivity of the material under wet conditions

The experimental technique for this test was identical to the one described in section 3.1. After the gas atmosphere and the surface of the reaction material had been saturated with water vapor, the autoclave was filled with hydrogen and the reaction rate was measured. Fig. 10 presents the results of these measurements. As one can see, the general shape of the curve has not been changed, but the initial reaction rate is significantly lower than in the dry case. This slowing down of the reaction cannot be the result of some chemical influence of the water on the surface of MnO_2, since from the previous results we concluded that water could even improve the reaction. Assuming that the material is covered by a thin water film, slowing down can be attributed to the rather low solubility of hydrogen in water and to the low diffusion rate of H_2 through the liquid. Although performances of the material deteriorate, both the reaction rate and capacity of the material are high enough for the application of the material as a hydrogen absorber under wet conditions.

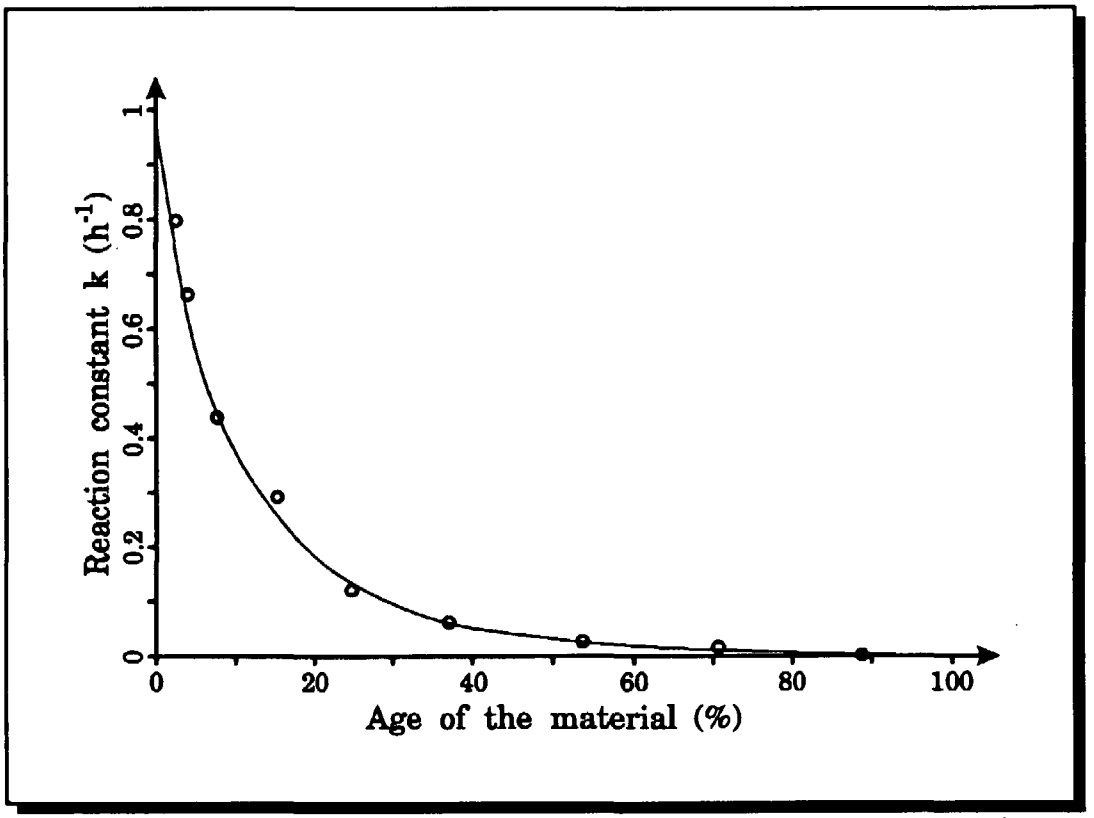

Fig.10. The reaction rate constant as a function of the reference materials' age under wet conditions.

4.2. Reactivity of the material in contact with salt

One of the possible ways of applying a hydrogen absorber in the final repository is to mix the reaction material with the crushed salt and use that mixture for back-filling the free space between the waste packages and walls of the emplacement borehole. The determination of any possible influence of the crushed salt on the reactivity of material was carried out using mixtures containing 2% of the reaction material. One of the mixtures was prepared using crushed salt in a form available from the Asse salt mine (Germany) containing about 0.03% humidity. The other was prepared using previously dried salt of the same origin. Fig. 11 depicts the reaction rate constants determined with these two materials. As one can see, in the case of natural salt the reaction stopped before reaching an age of 5%. Keeping in mind the fact that salt containing a certain amount of humidity rapidly undergoes the sintering process, the reaction may be stopped by that effect. Incorporation of

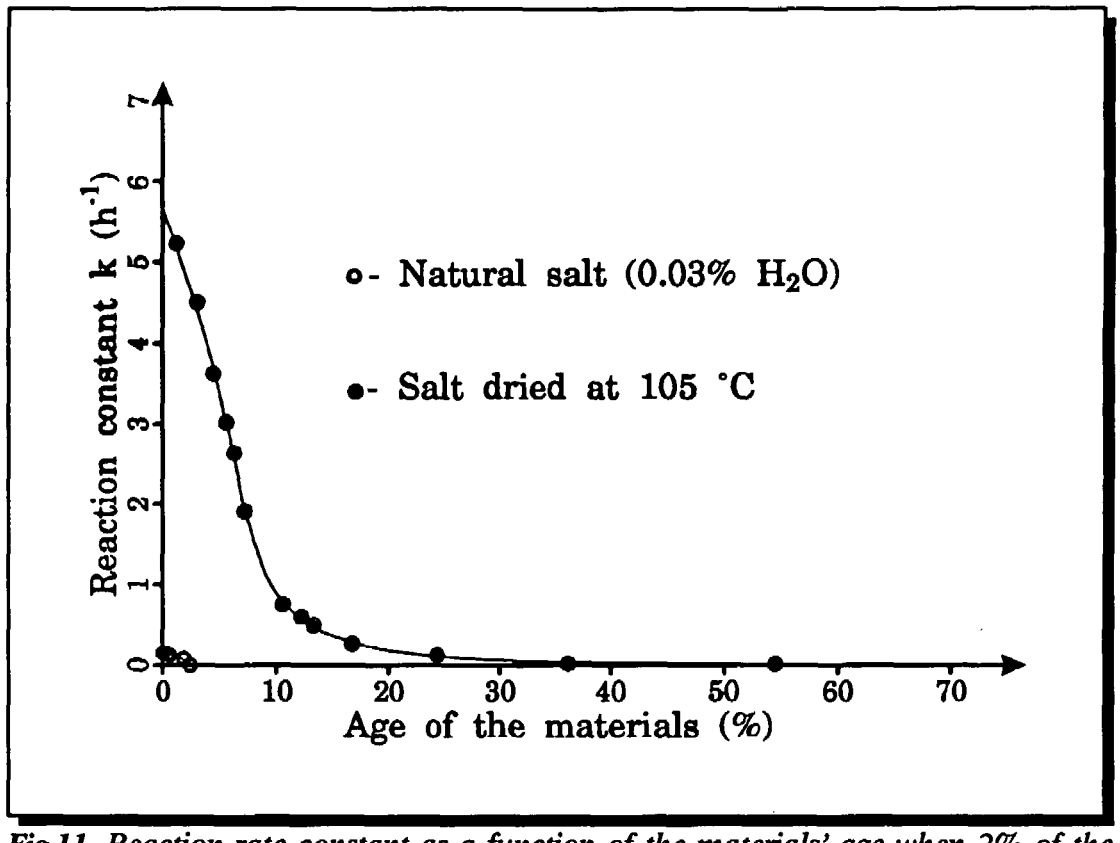

Fig.11. Reaction rate constant as a function of the materials' age when 2% of the reaction material was mixed with natural or previously dried crushed salt.

the fine powder of the reaction material in the sintered salt structure prevents any further contact with gaseous hydrogen and the reaction cannot proceed. Therefore, the amount of the reacted material depends on the humidity of the salt and on the time allowed for the sintering process. The results obtained with previously dried salt seem to support these conclusions. At the beginning, the reaction occurred quite normally until enough water was formed (as a reaction product) so that the sintering process could start. After that the reaction rate decreased rapidly and finally stopped before all the available capacity of the material was exhausted.

From these experiments it can be concluded that the application of any pulverized hydrogen absorber mixed with crushed salt will result in incorporation of the reaction material in the sintered salt structure preventing contact between hydrogen and reaction material. One of the possible technical solutions to this problem is the insertion of special containers holding the reaction material into the borehole after every 10 or 15 waste packages. This technique will prevent contact

between the humid salt and the bulk of the reaction material so that just a small fraction will be deactivated.

4.3. Reactivity of the material poisoned with NaCl and Na_2S

It is known that the gas phase of the pore system of the rock salt contains a small amount of H_2S and HCl. Since these gases can react with Ag_2O in the presence of humidity according to the reactions

$$Ag_2O + 2Cl^- + 2H^+ \rightarrow 2AgCl + H_2O \qquad \text{(Eq. 15)}$$

and

$$Ag_2O + S^{2-} + 2H^+ \rightarrow Ag_2S + H_2O\ , \qquad \text{(Eq. 16)}$$

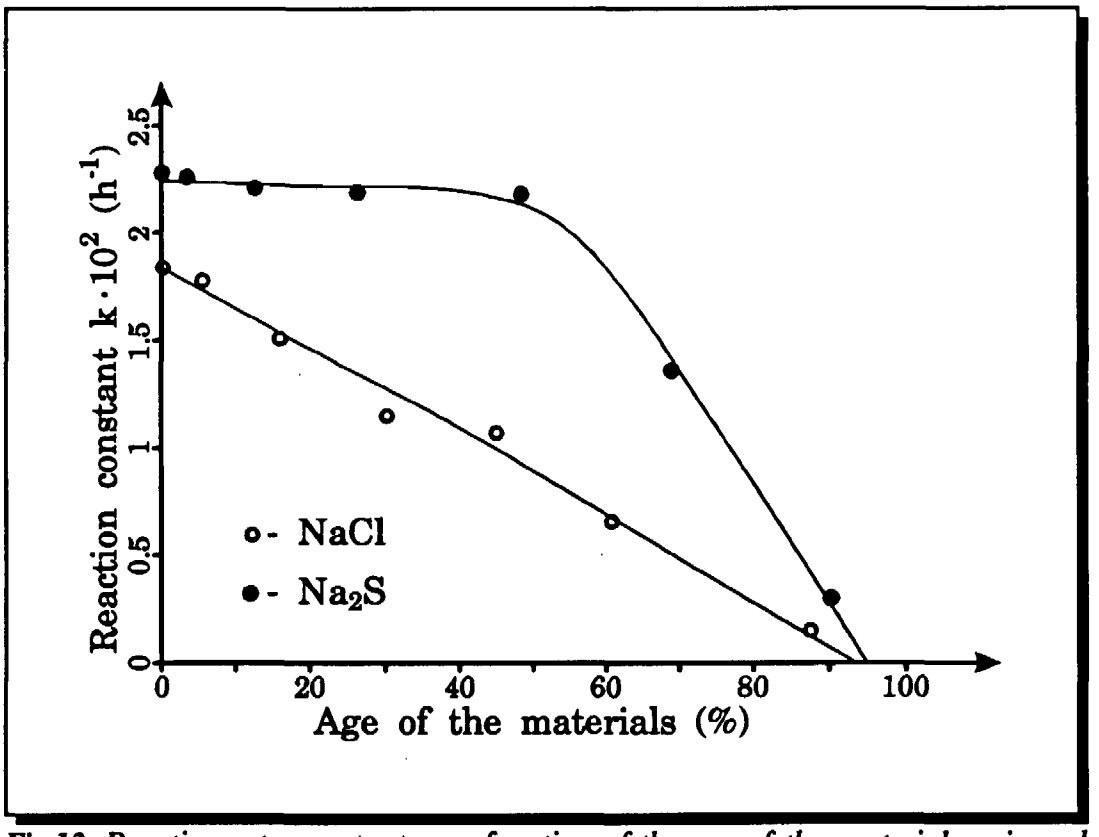

Fig.12. Reaction rate constant as a function of the age of the materials poisoned with NaCl and Na_2S.

it is necessary to determine the catalytic activity of AgCl and Ag_2S. Two equal samples of the reference material were equilibrated with saturated solutions of NaCl and Na_2S for 48 hours. The samples were then washed several times with distilled water and finally dried at 105 °C for 4 hours. Then, the reactivity of these samples was determined using the usual procedure. From fig. 12 one can see that the curves representing the reaction rate constant as a function of the materials' age are quite unusual but, although very slow, the reaction is still evident. Fig. 12 proves that AgCl and Ag_2S can have some catalytic effect as well as almost any silver compound[5]. The capacities of these materials are around 90% and one can conclude that the most serious effect of poisoning the catalyst is a very much decreased reaction rate. According to our calculations reported elsewhere[8], the measured initial reaction rates of both NaCl- and Na_2S-poisoned material are still two orders of magnitude higher than necessary to keep the hydrogen partial pressure below the safe value.

4.4. Radiolytic stability of the reaction material

The determination of the radiolytic stability of the material was carried out by γ-irradiation of a sample containing 10% Ag_2O prepared by powder mixing with electrolytic MnO_2. 590 g of this material was filled in a glass ampule and closed after evacuation. The ampule was then irradiated up to γ-doses of 1 MGy for 27 days. After irradiation the ampule was inserted in a special container, the container was evacuated and filled with N_2 up to a pressure of 2 bar. Then, the glass ampule was broken and the container was left overnight in order to obtain a homogeneous mixture of any possible radiolytically released gas with nitrogen. This gas atmosphere was then analyzed by a gas chromatograph (SICHROMAT 2, Simens). Although the Ag_2O concentration was very much increased in order to increase the sensitivity of this test for the radiolytic release of O_2, nothing was detected except N_2. From this finding one can conclude that both MnO_2 and Ag_2O are radiolytically stable compounds, which is common behavior for metallic oxides.

The reactivity of the material containing 10% Ag_2O was so high that it was impossible to measure the reaction rate using the same apparatus as for the materials containing about 1% Ag_2O. To prove that irradiation had no negative effect on the materials' reactivity, two experiments were performed using irradiated and nonirradiated materials in a 220 l stainless steel drum. 250 g of the reaction material, together with 250 g CaO as drying reagent, was filled in a sintered stainless steel cartridge and inserted inside a thermostated (110 °C) drum. The drum was then evacuated and refilled with pure nitrogen up to 900 mbar. Then, from a calibrated gas sack 10.9 l (STP) of hydrogen was sucked into the drum and the hydrogen concentration was measured by a hydrogen detector (Hydros 100, Leybold Haeraus) as a function of time. Fig. 13 shows the results obtained by nonirradiated

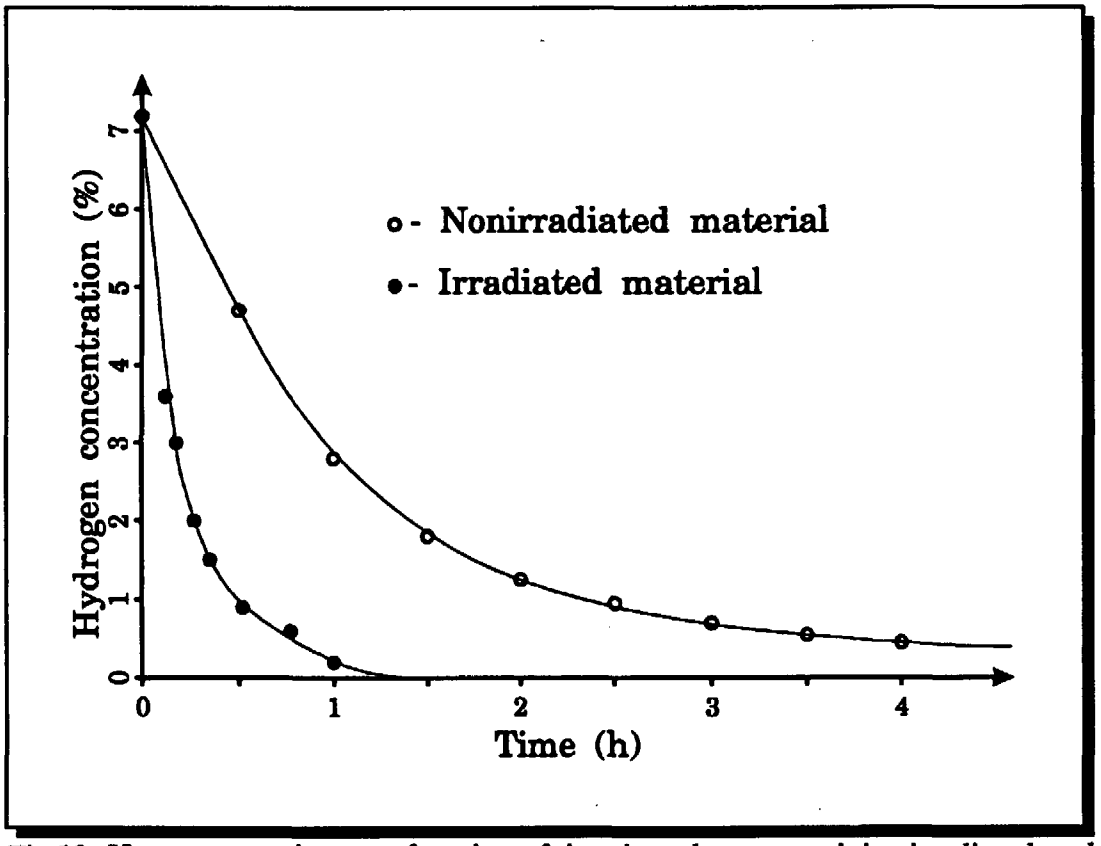

Fig.13. H_2 concentration as a function of time in a drum containing irradiated and nonirradiated reaction material.

(circles) and irradiated material (solid circles). As one can see, the irradiated material reacted even faster than the nonirradiated. Possibly, the dislocated electrons in the MnO_2 crystals resulting from the γ-irradiation could have some positive effect on the transport of hydrogen radicals in the bulk of the material increasing the reaction rate. After all the hydrogen from the drum was consumed, it was refilled with the same amount of H_2. This procedure was repeated until the reaction stopped. The total amount of hydrogen consumed by both irradiated and non-irradiated materials was equal to the reduction of MnO_2 to MnO (or H_2MnO_2) which corresponded to an age of 200%, meaning that the irradiation of the material had no negative effects on the materials' capacity. These results lead to the conclusion that the material can be applied as a hydrogen absorber even in high radiation fields.

4.5. Testing of the material in 200 l geometry

In the previous chapters it was shown that the selected reaction material can meet all the requirements for its application in the final repository. The goal of the experiments described below was to demonstrate the effectiveness of hydrogen absorption on a large scale, simulating the conditions in a segment of a real disposal borehole.

A 200 l drum was filled with crushed salt and thermostated to 50 °C. A cartridge consisting of a 41.5 cm long stainless steel tube having an inner diameter of 25 cm and volume of 20 l, closed from both sides with a sandwich of grid - glasswool - grid, was placed in the middle of the drum. During the preliminary experiments this cartridge was empty, later on it was filled with the hydrogen-absorbing material. Several capillary tubes were placed at various locations inside the drum, in order to take gas samples from different points. The temperature was monitored at two places inside and on the surface of the drum. The experimental set-up is shown in figs. 14 and 15. It was possible to evacuate the filled drum to ~ 50 mbar within 10 min by the use of a mechanical vacuum pump. At the bottom of the drum there was a gas inlet through a stainless steel tube with an inner diameter

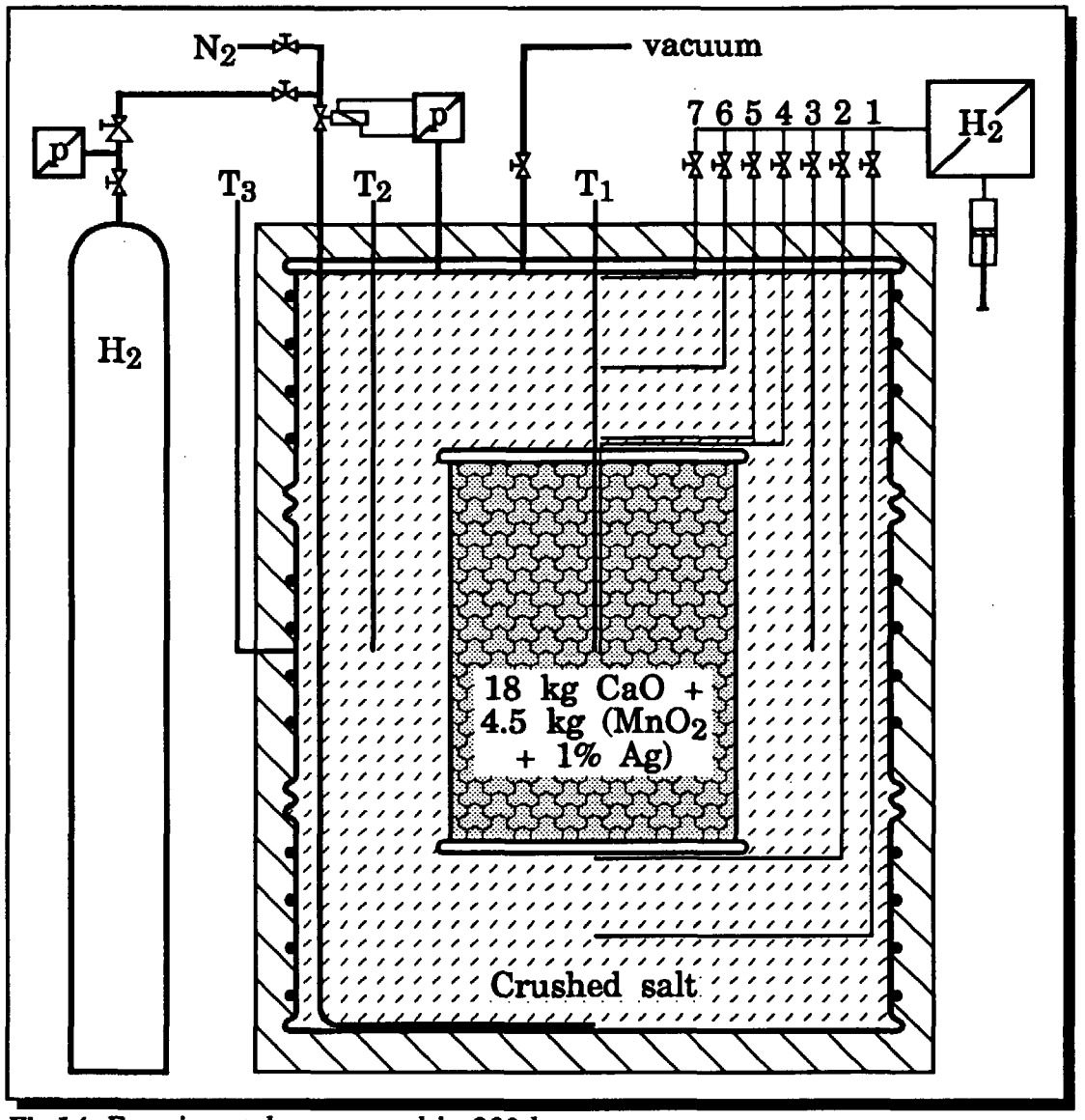

Fig.14. Experimental set-up used in 200 l geometry test.

of 4.5 mm. It was possible to feed H_2 or N_2 into the drum through a magnetic valve. The pressure of both gases was adjusted to 1.5 bar in front of this valve. The opening and closing of the magnetic valve was regulated by a mercury manometer with two built-in platinum contacts. As a result, it was always possible to refill the drum after evacuation with the selected gas to the same desired pressure, with a reproducibility of 0.2 mbar. On the other hand, with a gas sink inside the drum, the missing gas was replaced instantly (by automatic opening of the magnetic valve) holding the pressure inside the drum at the same level with an accuracy of ± 0.3

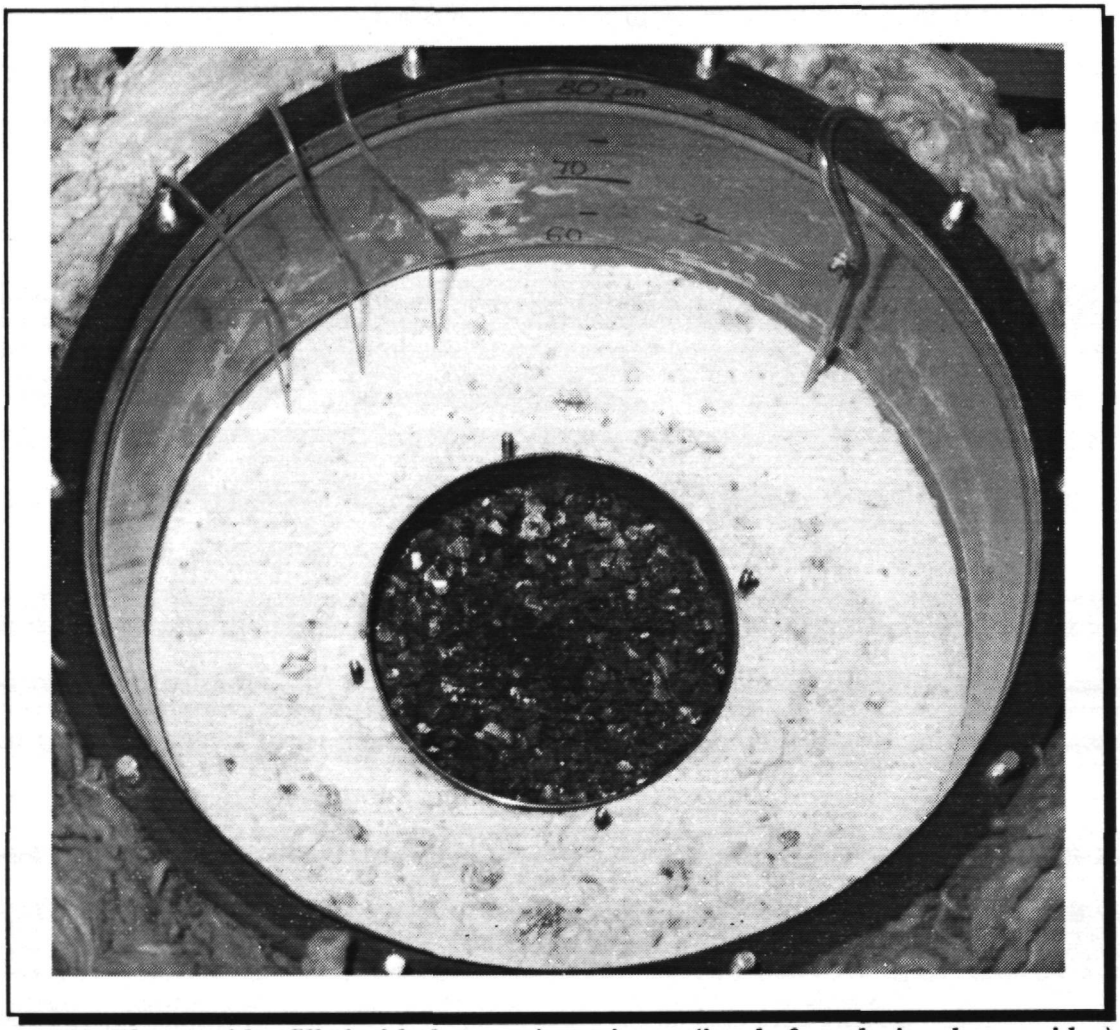

Fig.15. *The cartridge filled with the reaction mixture (just before closing the cartridge) emplaced in the crushed salt. Three of the seven capillary tubes and the gas inlet (wider tube) are visible.*

mbar.

The hydrogen concentration at different points inside the drum was measured by a hydrogen detector (Hydros 100, Leybold Haeraus). The detector was connected to the desired capillary tube and 10 ml of the gas was sucked through the measuring chamber by a gas-tight syringe. 15 sec after stopping the gas flow through the chamber, a stable reading was obtained and the gas was forced back into the drum with the same syringe.

In the first experiment, the diffusion rate of hydrogen through the crushed salt was examined with an empty cartridge inside the drum. The drum was

evacuated three times to 50 mbar and refilled to 1 bar with N_2 in order to remove the oxygen from the drum atmosphere. During the last filling, the pressure in the drum was adjusted to 954.7 mbar. The gas inlet was then switched to H_2 and the filling of the drum was completed with hydrogen to 1004.9 mbar total pressure, leading to an average H_2 concentration of 5.0% (by volume). Fig. 16 shows the H_2 distribution as a function of time (solid lines) at six different places. The numbers indicating the sampling points correspond to labels in fig. 14. It is evident that one hour after the H_2 injection a homogeneous distribution was obtained.

The second experiment was carried out in the same way as the one described above, except that the cartridge was filled with the reaction material. The content of the cartridge was a mixture of 4.5 kg activated MnO_2 (the reference material, described in ch. 4.) and 18 kg of CaO in form of small lumps (5-20 mm, Merck product 2109). According to current plans, the very same mixture could be used in the final repository as a hydrogen absorber. The role of CaO is threefold. First, thanks to relatively low density of the mixture (approx 1.25 $g \cdot cm^{-3}$ in contrast to the density of the activated MnO_2, amounting to 2.1 $g \cdot cm^{-3}$) the diffusion rate of gases through the material is increased. Second, CaO chemically binds water and therefore it will reduce the average humidity in the borehole, which might decrease the anoxic corrosion of the metallic parts emplaced in the repository. The third role of CaO was important only in the experiment described: CaO also bound the water vapor formed and thus the total pressure in the drum was the sum of N_2 and H_2 partial pressures only.

The results of this experiment are included in fig. 16 as dashed lines. It is obvious that the hydrogen uptake was very efficient. At every measuring point the H_2 concentration was far below the values without material in the cartridge. The total amount of hydrogen injected into the drum (about 5 l) was consumed within 3 hours. During all that time the H_2 concentration in the middle of the cartridge (measuring point 4) was less than the lower detection limit of the H_2 detector (0.1%). That means that the diffusion of hydrogen through the cartridge was much slower than the reaction rate.

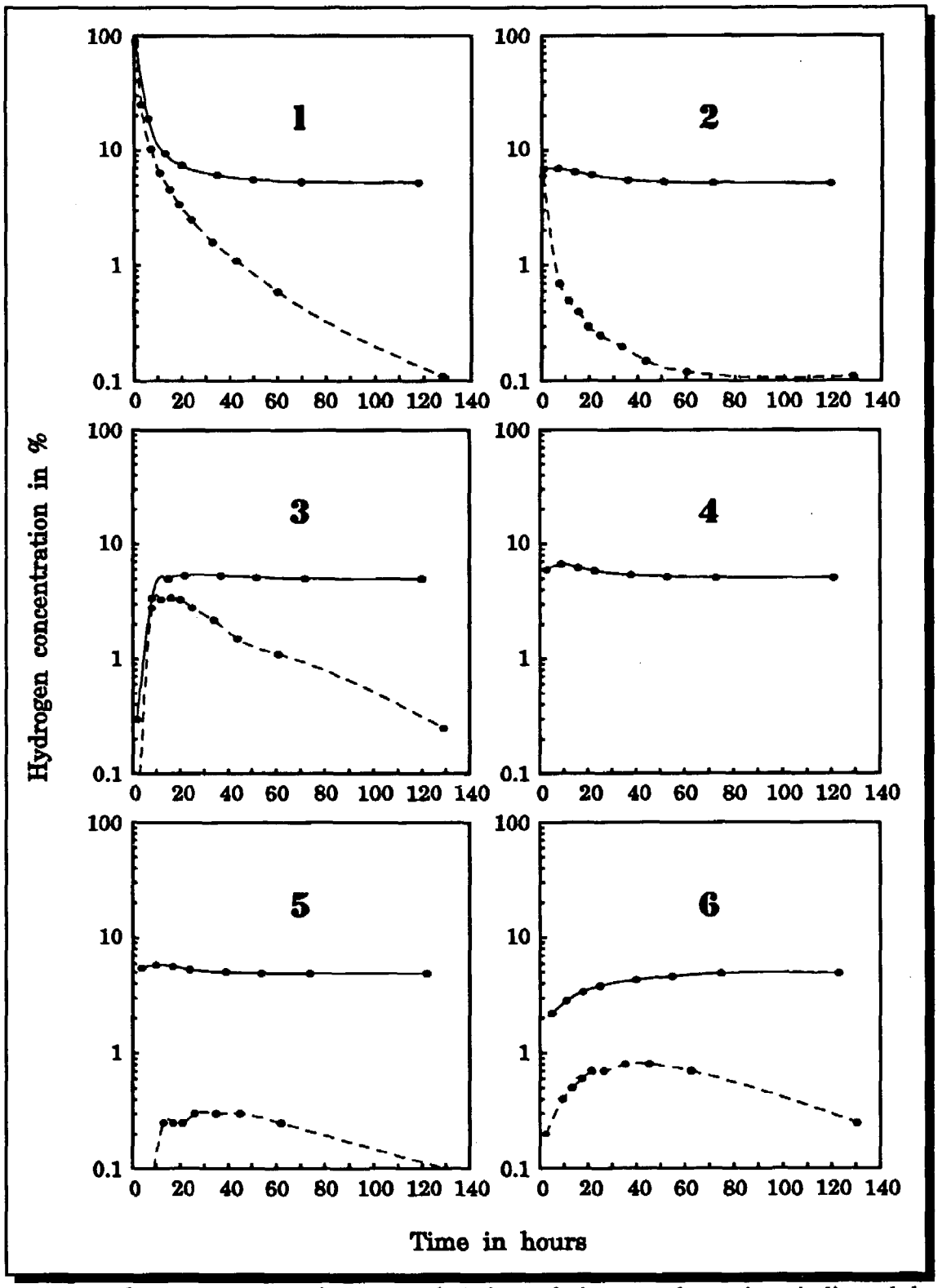

Fig.16. Hydrogen concentration as a function of time at the points indicated by numbers (according to fig. 14). Solid line - the cartridge is empty, dashed line - the cartridge is filled with the reaction mixture.

The third experiment was carried out with fresh material in the cartridge. The drum was again evacuated three times and refilled with N_2. The final pressure was adjusted to 954.7 mbar and then the gas inlet was switched to H_2. The source of the hydrogen was a 10 l high-pressure cylinder equipped with a pressure transducer (P42K/200, Hottinger Baldwin Messtechnik) operating in the range from 0 - 200 bar. At the starting point of the experiment the magnetic valve was opened and the drum was filled with H_2 from the initial pressure of 954.7 to 1004.9 mbar resulting in an average H_2 concentration of 5.0% and then it was closed automatically. Whenever the pressure in the drum decreased by more than 0.2 mbar, the valve was automatically opened and the missing H_2 (which had been reacted) was replaced from the hydrogen cylinder. In this way, the hydrogen absorption occurred at a constant average H_2 concentration of 5.0%. During the experiment, the H_2 pressure in the cylinder was recorded as a function of time. From the change of the H_2 pressure in the cylinder it was possible to calculate the

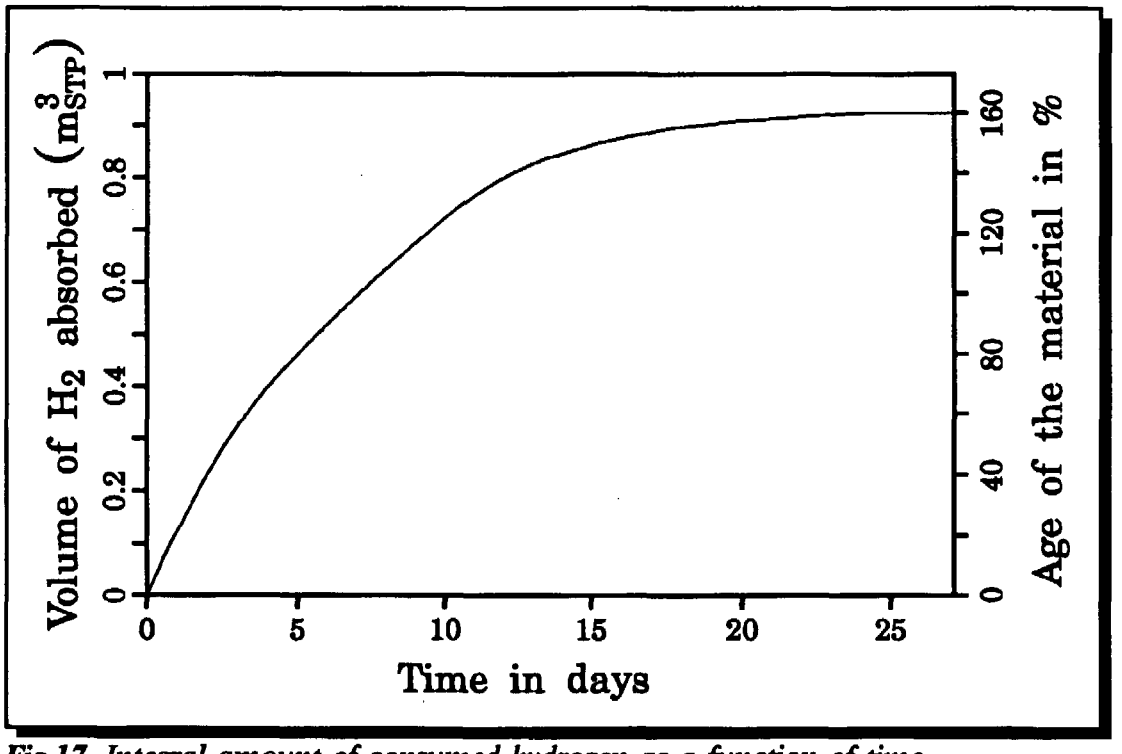

Fig.17. Integral amount of consumed hydrogen as a function of time.

amount of hydrogen already reacted, as well as the reaction rate as a function of time. Fig. 17 shows the integral amount of adsorbed H_2 during the experiment. During the first 5 days half of the total capacity of the material was consumed, whereas 90% of the available capacity was exhausted within the first 13.3 days. The experiment was canceled when there was no measurable H_2 uptake for 24 h. The final age of the material was calculated to be 160%, which is in excellent agreement with the results obtained in the small-scale experiments in autoclaves (see fig. 9). The temperature in the center of the cartridge is shown in fig. 18, while the measured reaction rate is depicted in fig. 19 as a function of the age of the MnO_2 (solid line). For comparison, the calculated reaction rate (not taking into account the diffusion rate and the changes of temperature) is included in fig. 19 (dashed line). Analyzing figs. 18 and 19, several conclusions can be drawn. At the beginning

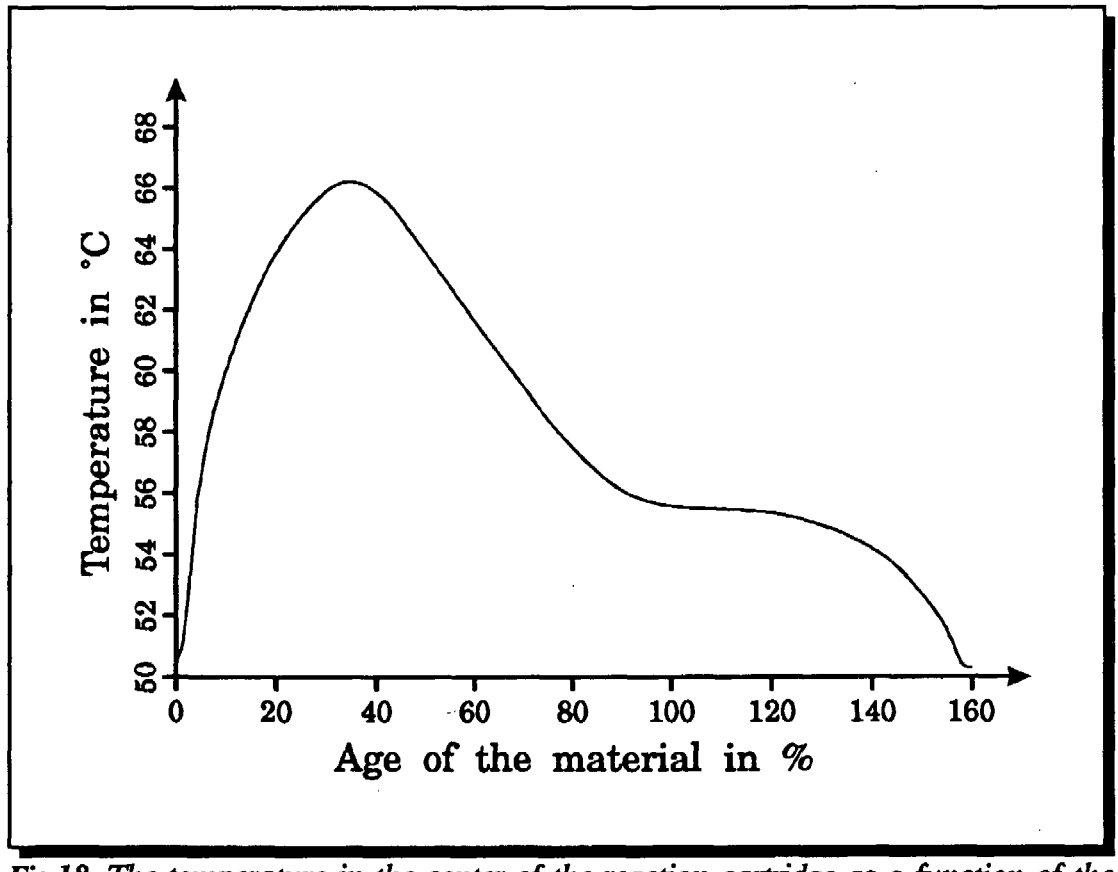

Fig.18. The temperature in the center of the reaction cartridge as a function of the age of the MnO_2

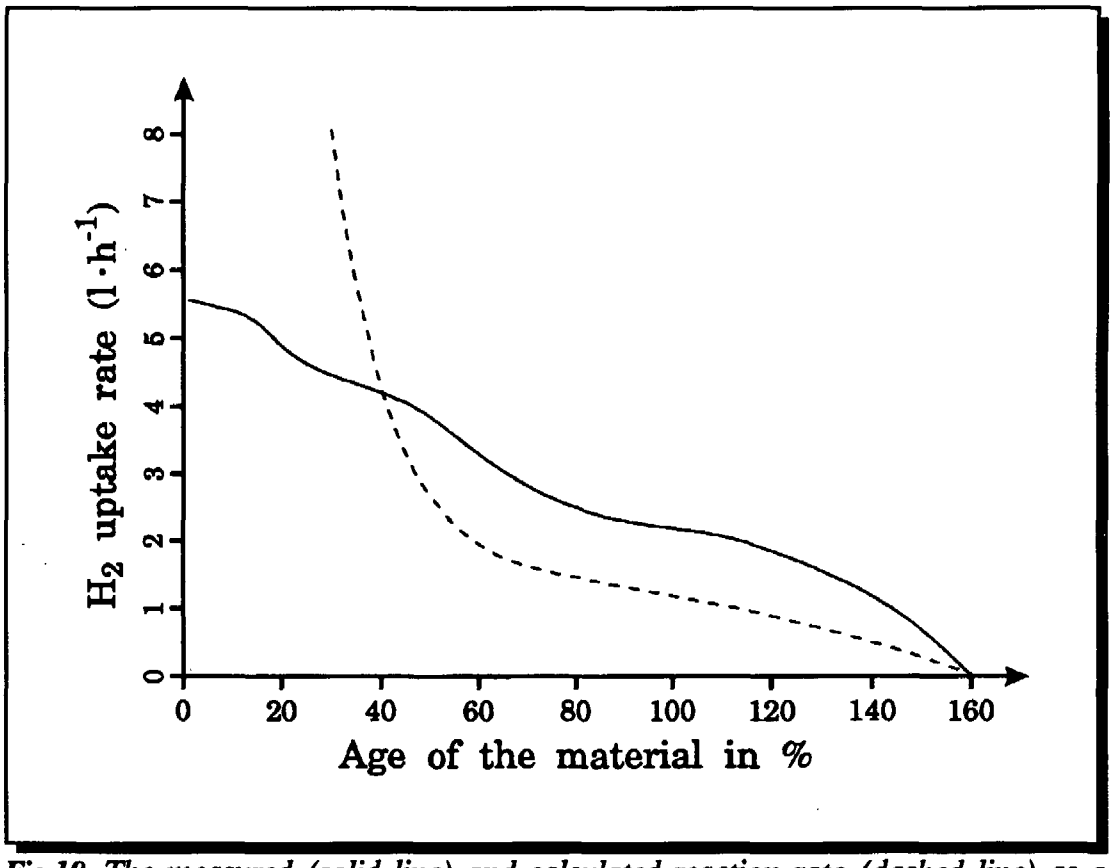

Fig.19. The measured (solid line) and calculated reaction rate (dashed line) as a function of the age of the MnO_2

of the reaction (speaking in terms of used capacity and not time), there was a high heat production, increasing the temperature from the initial 50.7 to the maximal 66.3 °C corresponding to the age of 35%. After that the temperature decreased to about 55 °C and it was almost constant between 90 and 120% age. Finally, the temperature of the reaction mixture dropped to the initial value. The complexity of the changes of temperature is a result of several factors acting in parallel. There were two heat sources in the cartridge: the reaction of H_2 oxidation resulting in water and the reaction between H_2O and CaO. The very high heat production at the beginning of the reaction is obviously the sum of the heat productions of both reactions. Bearing in mind that just a part of the hydrogen is really oxidized to water (on the surface of MnO_2 from where the water molecules can escape) and that the rest of H_2 is bound in the bulk of MnO_2 crystals, the decreased heat production after the age of 35% can be easily explained. The almost constant temperature in

the range from 90 to 120% age is a result of the difference between the heat production rate (binding of H_2 in the bulk of MnO_2) and the heat dissipation through the walls of the drum. Finally, at the end of the capacity of the materials the reaction was too slow to compensate for the heat dissipation and the temperature decreased to the initial level.

Comparing the measured and calculated reaction rates (fig. 19), it is obvious that at the beginning of the reaction the diffusion of H_2 through the reaction material is the limiting factor, since the reaction rate is about 100 times slower than it should be. At the same time, there was a great increase in temperature which could have increased the reaction rate if it were not controlled by diffusion. From approximately 40% of the materials' age the reaction rate was quite close to the calculated one, since the reaction was slow enough to be defined by the materials' behavior and not by diffusion. In the region from 50 to 160% of the age, the measured reaction rate was always higher than the calculated one, due to the increased temperature of the reaction material.

Extrapolating the results of the presented experiment to a real disposal borehole, one can conclude that except at the very beginning of the reaction (up to 40% of the materials' age or 25% of the materials' total capacity) where the reaction rate is controlled by diffusion of H_2 through the reaction material, the reaction rate is controlled by the behavior of the Ag-activated MnO_2 and of course by the diffusion of H_2 through the salt matrix. As shown in previous chapters, the proposed material can react at a sufficient rate even if humid and completely poisoned, leading us to the conclusion that the material can be efficiently used in the final repository as a hydrogen adsorber.

5. PROPOSED TECHNIQUE FOR HYDROGEN ABSORPTION IN THE FINAL REPOSITORY

This proposal is valid for the final disposal of COGEMA containers containing intermediate level radioactive waste in boreholes, but it can be easily adapted to every type of containers. Some important parameters of such a container are shown in table 1. From the operational point of view the simplest way to

Largest external diameter	*1.13 m*
Overall height	*1.71 m*
Weight of the empty container	*470 kg*
Weight of the full container	*3500 kg*
Inner volume	*1.3 m^3*
Radiolytic production of hydrogen	*6.7 m^3/100 years*
Hydrogen production by corrosion	*1.8 - 8.8 m^3/100 years*
Maximal expected hydrogen production	*15.5 m^3/100 years*

Table 1. Parameters of a COGEMA container[9]. Hydrogen production is estimated assuming a corrosion rate of 0.5-2.5 μm/year for stainless steel in the salt environment[8].

emplace the hydrogen absorption material in the borehole would be in some sort of container having outer dimensions and shape as close as possible to the parameters of a COGEMA container. These special containers should have perforated walls so that the hydrogen has access to the reaction material. Considering the parameters of the COGEMA container (table 1), such an absorption container would have an inner volume of about 1.3 m^3. At least 0.1 m^3 must be left empty in the container since CaO increases its volume during the reaction with water. The remaining 1.2 m^3 has to be filled with the reaction material

(1 : 4 mixture of Ag activated MnO_2 and CaO). That means that every absorption container will contain 300 kg of activated MnO_2 and 1200 kg of CaO. 300 kg of Ag-activated MnO_2 has an adsorption capacity of 62 m^3_{STP} of H_2, meaning that for every 4 COGEMA containers one absorption container should be emplaced. Assuming that all of this H_2 will be converted to H_2O (this is a conservative assumption, since part of the H_2 is directly bound in MnO_2), a maximum of 49.8 l H_2O will be produced in such an absorption container. 1200 kg of CaO has a total capacity for H_2O absorption of 385.7 l. It is obvious that in every absorber container there is free capacity for absorption of an additional 335.9 l of H_2O in the form of brine in the rock salt.

Considering a segment of the borehole containing 4 COGEMA and 1 absorption containers as described above and repeating the calculation procedure described elsewhere[8], one can see that during the first 100 years there will be no significant H_2 pressure build-up. If the amount of incoming humidity into this segment of the borehole is less than 3.3 l H_2O/year the overall humidity in the segment will be significantly reduced, thus minimizing the anoxic corrosion of the metallic parts of the containers and reducing the H_2 production.

6. CONCLUSION

MnO_2 catalytically activated by Ag_2O was tested as a candidate material for hydrogen absorption in the final repository. The catalytic activation of the MnO_2 was achieved by using three techniques: powder mixing, chemical deposition of Ag_2O on the surface of MnO_2 and ion exchange deposition of Ag^+ on the surface of electrolytically prepared MnO_2.

Materials based on natural MnO_2 (pyrolusite, brownstone) cannot react under wet conditions and are therefore not suitable for application in the final repository.

Since the contact surface between the Ag_2O and MnO_2 particles is rather low after simply mixing the powders, this material proved to be inferior compared to the materials prepared by ion exchange.

It is confirmed that the fastest reaction with hydrogen is with the material (based on electrolytical MnO_2) prepared by ion exchange, treated by NaOH solution and dried in vacuum at room temperature. Although the same material dried at 105 °C has a somewhat lower initial reaction rate, this material was selected for testing under repository-relevant conditions since this drying technique is more common on an industrial scale. The material can react with hydrogen even when the gas atmosphere and the materials' surface are saturated with water. Also, the material can react when the catalyst is completely poisoned and transformed to AgCl or Ag_2S. Testing of the material γ-irradiated up to a dose of 1 MGy proved that irradiation had no negative effect either on the materials' reactivity or on the total capacity for hydrogen absorption.

Mixing of the reaction material with slightly humid crushed salt will result in incorporation of the material in the sintered salt structure preventing any contact with hydrogen. For the application of this material as a hydrogen absorber in the final repository, it must therefore be ensured that the reaction material is emplaced in the borehole in a discrete form in special containers.

It was shown by a 200 l scale experiment that placing the reaction material in a discrete form (in a 20 l cartridge) in the salt environment results in very efficient hydrogen absorption, confirming that the proposed technique can be applied in a real final repository.

7. ACKNOWLEDGEMENTS

The author is grateful to Mr. H. Vijgen for ICP measurements and to Dr. B.-G. Brodda for gas-chromatographic analyses. Special thanks to Dr H. Brücher and Dr K. Kroth for invaluable discussions and hints.

8. REFERENCES

[1] K. Kroth, E. Barnert, P.H. Brücher, H. Lammertz, D. Niephaus, Waste Management '90, Int. Symp., 25. 02. - 01. 03. 1990, Tucson, Arizona, p.363.

[2] K. Kroth, H. Lammertz, "Radiolytische Bildung von Wasserstoff in Proben von homogen zementiertem Feedklärschlamm", **Jül-Spez-2401**, KFA Jülich, 1990.

[3] "Möglichkeiten der Beseitigung von Radiolysewasserstoff in Abfallbehältern mit Filterkerzen aus der Brennelementreinigung", Arbeitsbericht **WTI/BAG/01/87**, Wissenschaftlich-Technische Ingenieurberatung GmbH, Titz-Rödingen, 1987.

[4] H. Lammertz, K. Kroth, "Untersuchungen zur Vermeidung der Bildung von Radiolyse-Wasserstoff in 200-l-Fässern mit zementiertem wärmeentwickelndem MAW aus der WAK", **Jül-Spez-430**, KFA Jülich, 1988.

[5] A. Kozawa and K.V. Kordesch, Electrochimica Acta, **26** (1981) 1489.

[6] J. Brenet, P. Chartier. M.-T. Dott, M. Gross, K. le Tran, K. Traore, Electrochim. Acta, **13** (1968) 2167.

[7] A. Kozawa, J. Electrochem. Soc., **106** (1959) 552.

[8] J.J. Čomor, K. Kroth, "Technical Proposal to Consume Hydrogen During its Production in a Final Repository", **ICT-TB-04/91**, KFA Jülich, 1991.

[9] Specifications for Cemented Waste (Hulls and End Caps) Produced by Plants UP2 800 and UP3 at La Hague, COGEMA, Mar. 1990.